

Quantitative imaging datasets of surface micro to mesoplankton communities and microplastic across the Pacific and North Atlantic Ocean from the Tara Pacific Expedition

a supprimé: surface

Zoé Mériquet¹, Guillaume Bourdin², Nathaniel Kristan², Laetitia Jalabert³, Olivier Bun¹, Marc Picheral³, Louis Caray-Counil¹, Juliette Maury¹, Maria-Luiza Pedrotti¹, Amanda Elineau³, David A. Paz-Garcia⁴, Lee Karp-Boss², Gaby Gorsky¹, Fabien Lombard¹ and Tara Pacific Consortium Coordinators team^{*}

¹Laboratoire d'Océanographie de Villefranche-sur-Mer, Sorbonne Université, CNRS, France

²School of Marine Sciences, University of Maine, Orono, Maine 04401, USA

³Sorbonne Université, CNRS, Institut de la Mer de Villefranche, IMEV, 06230 Villefranche-sur-Mer, France

⁴Laboratorio de Genética para la Conservación, Centro de Investigaciones Biológicas del Noroeste, Baja California Sur 23096, México.

^{*}A full list of authors appears at the end of the paper.

Correspondence to: Zoé Mériquet (zoe.meriguat@imev-mer.fr) and Fabien Lombard (fabien.lombard@imev-mer.fr)

Abstract. This paper presents the quantitative imaging datasets collected during the Tara Pacific Expedition (2016-2018) on the schooner Tara. The datasets cover a wide range of plankton sizes, from micro-phytoplankton > 20 μm to meso-zooplankton of a few cm, as well as non-living particles such as plastic and detrital particles. It consists of surface samples collected across the North Atlantic and the North and South Pacific Ocean from open ocean stations (a total of 357 samples) and from stations located in coastal waters, lagoons or reefs of 32 Pacific islands (a total of 228 samples). As this expedition involved long distances and long sailing times, we designed two sampling systems to collect plankton while sailing at speeds up to 9 knots. To sample microplankton, surface water was pumped onboard using a customised pumping system and filtered through a 20 μm mesh size plankton net (here after Deck-Net (DN)). A High Speed Net (HSN; 330 μm mesh size) was developed to sample the mesoplankton. In addition, a Manta net (330 μm) was also used when possible, to collect mesoplankton and plastics simultaneously. We could not deploy these nets in reef and lagoon stations of islands. Instead, two Bongo nets (20 μm) attached to an underwater scooter were used to sample microplankton. In addition to describing and presenting the datasets, the complementary aim of this paper is to investigate and quantify the potential sampling biases associated with these two high speed sampling systems and the different net types, in order to improve further ecological interpretations. Regarding the imaging techniques, microplankton (20-200 μm) from the DN and Bongo nets was imaged directly on-board Tara using the FlowCam (Fluid imaging, Inc.) while the mesoplankton (> 200 μm) from the HSN and Manta nets was analyzed in the laboratory with the ZooScan system, back on land. Organisms and other particles were taxonomically and morphologically classified using the web application EcoTaxa automatic sorting tools, followed by taxonomic expert validation or correction. For microplankton smaller than 45 μm , a subsample of 30% of the annotations was 100% visually validated by experts. More than 300 different taxonomic and morphological groups were identified. The datasets include the metadata with the raw data from which morphological traits such as size (ESD) and biovolume have been calculated for each particle, as well as a number of quantitative descriptors of the surface plankton communities. These include abundance, biovolumes, Shannon diversity index and normalised biovolume size spectra, allowing the study of their structures (e.g. taxonomic, functional, size structure, trophic structure, etc.) according to a wide range of environmental parameters at the basin scale.

a supprimé: Microplankton

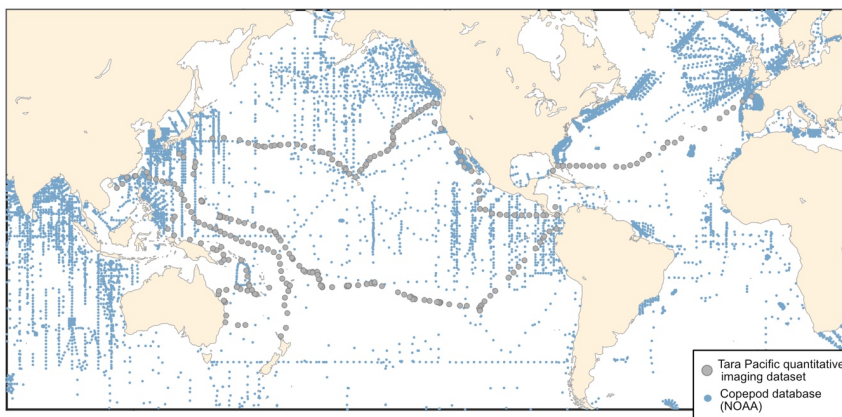
a supprimé: In addition to describing and presenting the datasets, the complementary aim of this paper is to investigate and quantify the potential sampling biases associated with the two high speed sampling systems and the different net types, in order to improve further ecological interpretations.

a mis en forme : Anglais (G.B.)

1. Introduction

53 Zooplankton serve as an important conduit for the transfer of energy from primary producers to higher trophic
 54 levels (Ikeda, 1985). In this key position in the food webs, they also play an important ecological and
 55 biogeochemical role (Turner, 2015; Steinberg and Landry, 2017), with associated ecosystem services. In
 56 particular, they are essential to Pacific fisheries management, as they influence fish productivity and ecosystem
 57 dynamics (Balachandran and Peter, 1987; Chuanbo Guo et al., 2019; Hays, 2005). The datasets we present here,
 58 cover a wide diversity of surface plankton, ranging from 20 μm to few cm, at the scale of the Pacific Ocean. The
 59 vastness and unique characteristics of the Pacific Ocean make it a particularly interesting study area. From
 60 nutrient-rich upwelling or islands zones to oligotrophic gyres, the diverse oceanic processes of the Pacific Ocean
 61 present a wide range of environmental conditions that significantly influence plankton communities, making it a
 62 key region for plankton research (Chavez et al., 2011; Longhurst, 2007). However, sampling efforts of
 63 zooplankton in the Pacific Ocean largely focused on the temperate North Pacific, eastern and western boundary
 64 currents in the North Pacific, leaving vast areas under-sampled (Drago et al., 2022). This gap is particularly evident
 65 in the NOAA zooplankton dataset (<https://www.st.nmfs.noaa.gov/copepod/atlas>), where the under-sampling is
 66 particularly true for the central subtropical and tropical Pacific where fisheries are important resources for the
 67 thousands of pacific islands. We present a map (Fig. 1) overlaying updated zooplankton databases with samples
 68 from the Tara Pacific expedition, illustrating how these new data address sampling gaps. Global mapping of
 69 zooplankton in the Pacific is hindered by the highly expansive operational ship time face to this vast ocean. The
 70 use of high-speed sampling, such as the Continuous Plankton Recorder (CPR, by Hardy in 1926), the LHPR
 71 (Longhurst et al., 1966), the Gulf III OCEAN Sampler (Gehring, 1958), the Gulf V plankton sampler (Sameoto
 72 et al., 2000), as well as newer low-tech designs (CSN in Von Ammon et al., 2020; Coryphaena in Mériquet et al.,
 73 2022), including the one employed in our datasets, provides valuable opportunities to expand sampling coverage
 74 and frequency and thus address this undersampling. In the hope of increasing similar cruising speed zooplankton
 75 sampling efforts, we discuss the benefits, challenges and limitations of this high-speed sampling approach based
 76 on the lessons learned from obtaining these datasets.

- a supprimé: trophic chain
- a supprimé: socio-economic interests
- a supprimé: .
- a supprimé: propose
- a supprimé: s
- a supprimé: size
- a supprimé: rich



78
 79
 80 **Figure 1. Spatial distribution of zooplankton observations from the COPEPOD database**
 81 **(<https://www.st.nmfs.noaa.gov/copepod/>; all groups) is represented by blue points. Plankton imaging data (> 20 μm)**
 82 **from the Tara Pacific expedition are shown in grey.**

83
 84 The aim of this paper is therefore to present and discuss this open-access quantitative plankton imaging datasets
 85 sampled during the Tara Pacific Expedition (2016-2018), conducted in the Pacific Ocean. In general, the effects
 86 of different environmental forcings on plankton are often focusing on one size range of plankton, or on a particular
 87 taxonomic or functional type to the exclusion of others. It is often difficult to reconcile different methods of

95 analysis (taxonomic, biogeochemical, genomic) to provide a coherent view of the plankton as a whole. In this
96 respect, quantitative imaging is complementary to other methods to study plankton community composition (e.g.
97 HPLC, flow cytometry, genomics) because it simultaneously provides quantitative measures of abundance,
98 morphology and biovolume (as a proxy for biomass) for different taxonomic groups of plankton organisms
99 (Lombard et al., 2019). The datasets represent a diversity of surface plankton analysed with the use of two
100 quantitative imaging instruments: 1. the FlowCam (Sieracki et al., 1998), which images microplankton from 20
101 to 200 µm, and 2. the ZooScan (Gorsky et al., 2010), which images meso-zooplankton (>200 µm). The dataset
102 also includes the plastics imaged by the ZooScan. Overall, it encompasses a total of 2 356 231 images, including
103 both surface micro and mesoplankton, as well as non-living particles such as plastics, making a significant
104 contribution to improving the availability of plankton data.

106 These datasets are of great value because of the relative rarity of sampling surface planktonic communities at the
107 oceanic scale. Potential limitations of the data presented here are discussed below. To ensure adequate spatial
108 coverage while considering navigation constraints, we designed two new sampling systems to collect surface
109 micro- and mesoplankton while sailing at a maximum speed of 9 knots. The 'Dolphin' sampler was designed to
110 pump seawater into a 20 µm net on board, the Deck Net (DN), while the 'High Speed Net' (HSN) was designed
111 and towed to collect surface plankton larger than 300 µm in size (see Gorsky et al., 2019 for details). In addition
112 to these high-speed sampling devices, but with less extensive spatio-temporal coverage, a Manta net (330 µm)
113 was also used whenever cruising speed made it possible (i.e. < 4 knots), to collect surface mesoplankton and
114 plastics. Two Bongo nets (20 µm), towed by an underwater scooter, were also used by scuba divers around islands,
115 reefs, and lagoons. Thus, a complementary objective of this paper is study and quantify the potential sampling
116 biases of the different methods used during this expedition, in order to maximize the quality of the data offered to
117 the scientific community and promote similar high speed zooplankton sampling efforts which strongly enhance
118 the spatial coverage of samples. Another characteristic of these datasets is the daytime sampling of surface (0-1
119 meter) plankton communities. This offers the possibility of geographic intercomparisons and interdisciplinary
120 studies related to the ocean's surface layer, enabling direct comparisons with other surface measurements, such as
121 satellite and atmospheric data. However, this raises questions about the quantitative nature of the sampling itself,
122 particularly regarding the representativeness of the datasets. While these datasets provide quantitative accuracy
123 by offering all the necessary information to consistently calculate estimates of the sample contents, we must warn
124 that the data may not fully be 'quantitatively representative' of the broader ecosystem. Although the sampling
125 objective is the surface layer, daytime sampling alone cannot document the nocturnal intrusion of migrating
126 zooplankton and micronekton to the surface. It is worth mentioning that night sampling was also operated on
127 zooplankton alone (see Fig 10 in Gorsky et al 2021) but therefore does not reconcile in space and time with day
128 sampling and was therefore not analyzed in priority.

129 2. Methods

130 2.1 Sampling

131 We present a collection of FlowCam and ZooScan images acquired during the Tara Pacific expedition (2016-
132 2018; Gorsky et al. 2019, Lombard et al. 2023). All samples and protocol names in this article follow Lombard et
133 al. (2023) in order to help the user match the samples and associated data presented here with other samples from
134 the expedition. Sampling was carried out generally at the daily frequency, every ~150-200 nautical miles, during
135 daytime, resulting in a total of 249 sampling events labelled [oa001] to [oa249] (Fig. 2). The first 28 sampling
136 events occurred during the trans-Atlantic crossing as the ship sailed from France to the Pacific. At the end of the
137 expedition, the schooner Tara acquired quantitative imaging samples at stations [oa232] to [oa249] across the
138 North Atlantic. Data are published on the SEANOE platform to allow for future updates and completion of
139 datasets. The plankton sampling covers a large latitudinal range (temperate, subtropical, and tropical) as well as a
140 diversity of environments associated with different oceanic regimes (equatorial upwelling, coastal upwelling,
141 eastern boundary current, subtropical gyres, and other provinces). We collected over 357 samples in the open
142 ocean and 228 samples close to the reef or in the lagoon. A selection of 32 coral reef islands systems (labelled

a supprimé: , Mériquet et al., 2022

a supprimé: The datasets

a supprimé: represent

a supprimé: . As with previous Tara expeditions, organizing and cross-linking the various measurements is a stepping-stone for true open access science resources following FAIR principles (Findable Accessible Interoperable and Reusable; Wilkinson et al. 2016). In this effort, the strategy adopted by Tara Pacific is to provide open access data and early and full releases of the datasets once validated or published. All the samples that make up these datasets should expand the base of standardised data needed to study basin-scale processes in the Pacific Ocean. One of the more valuable aspects of the plankton sampling strategy of the Tara Pacific expedition, is the daily sampling, every ~150-200 nautical miles, crossing a large latitudinal range of different oceanic processes such as equatorial upwelling, coastal upwelling, eastern boundary current, subtropical gyres... The samples were collected around 32 coral reef islands or in lagoons and at 132 open ocean stations, traversing different oceanic provinces. We collected over 357 samples in the open ocean and 228 samples close to the reef or in the lagoon. This offers a potential avenue for exploring the impact of reef islands on plankton abundance and community structure, potentially shedding light on the still incompletely understood phenomenon of Islands Mass Effect (IME; Gove et al., 2016, Messié et al. 2022). In relation to the environmental data from the expedition, published in open access by Lombard et al. 2023, these datasets can be used for global ecological studies of the quantitative and qualitative aspects of planktonic communities at the basin-scale processes. ¶

a mis en forme : Police :italique

a supprimé: ¶

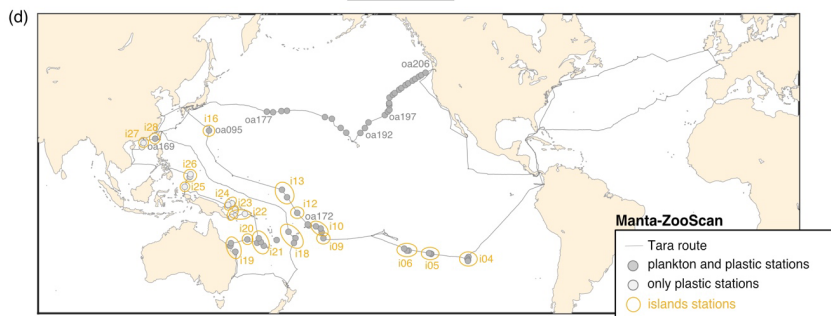
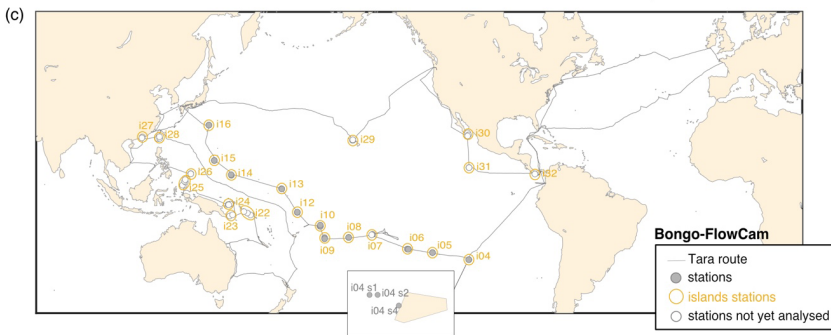
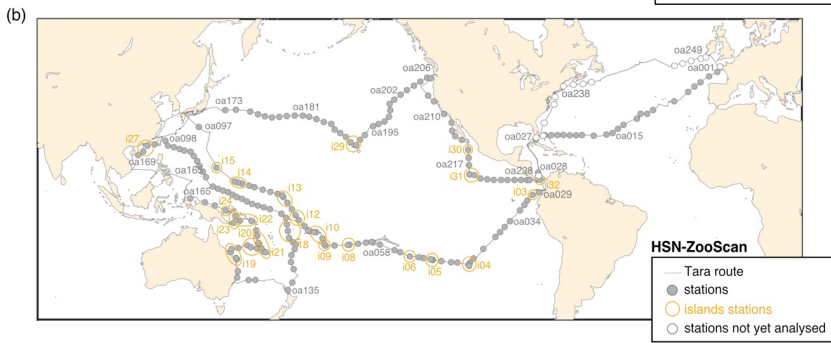
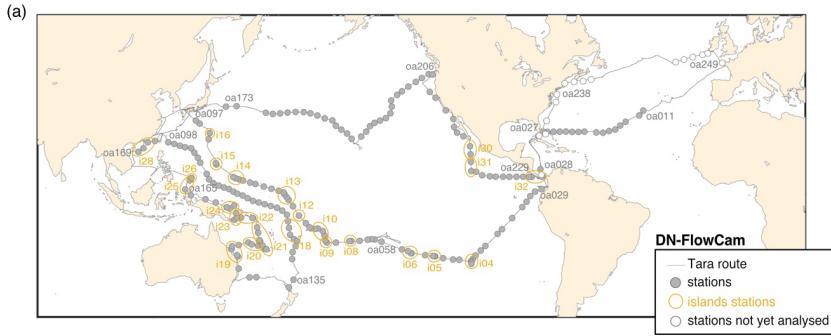
This 2-year expedition involved long distances and long sailing times, for which we designed two new sampling systems to collect surface plankton while sailing at a maximum speed of 9 knots. The 'Dolphin' sampler was designed to pump seawater into a 20 µm net on board, the deck net, while the 'High Speed Net' (HSN) was towed to collect surface plankton larger than 300 µm in size (see Gorsky et al., 2019 for details). In addition to these high-speed sampling devices, a Manta net (330 µm) was also used when possible, to collect mesoplankton and plastics simultaneously. The Manta and HSN nets must be towed relatively long distances to filter enough volume to provide quantitative estimates of plankton taxa in oligotrophic waters. The reef and lagoon configuration often did not allow such long towing distances with these devices, so we adapted the sampling strategy to lagoons using a Bongo frame fitted with two 20 µm Bongo nets towed by an underwater scooter. A complementary objective of this paper is to investigate and quantify potential sampling biases associated with the high-sampling devices and between each net type, in order to improve subsequent ecological interpretations and promote similar cruising speed zooplankton sampling efforts. ¶

a supprimé: processes

200 [i01] to [i32]) in the tropical and subtropical Pacific Ocean were targeted for coral reef holobiont studies (Planes
201 et al., 2019), including surface plankton sampling analysed by quantitative imaging. A summary of geological,
202 topological and human population characteristics of the different islands targeted (name, size, elevation, human
203 population, etc.) can be found in Lombard et al. (2023). Any sampling event that was conducted within the
204 Exclusive Economic Zone (EEZ) of an island (defined as the area that stretches 200 nautical miles or 370 km out
205 of the coastline of an island in question) was considered as an island station and annotated with the island label
206 [i##_oa###]. All other sampling events were considered open ocean stations (high seas, [132 open ocean stations](#))
207 and were annotated [i00_oa###].

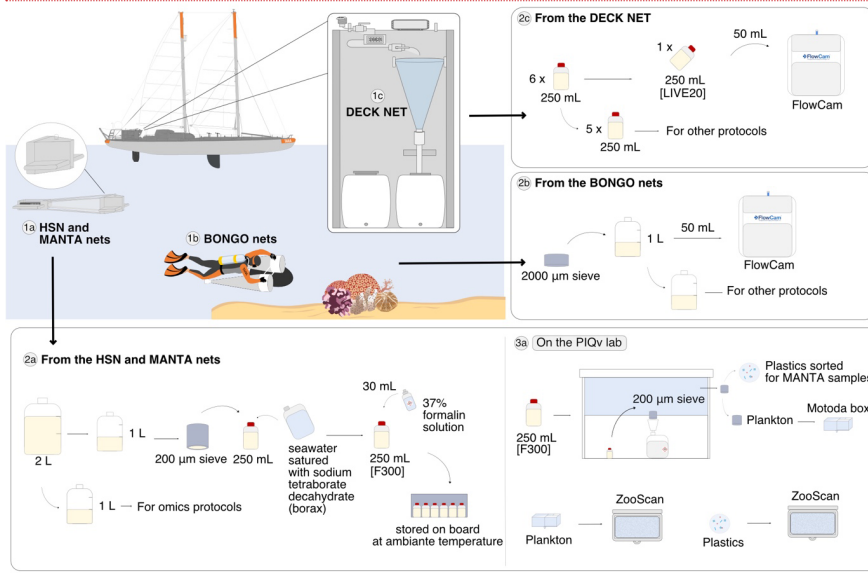
a supprimé: ¶

... [1]



212 Figure 2. Tara Pacific expedition (2016–2018) sampling map for the 4 different datasets. **Continuous sampling: (a) DN**
 213 **(Deck-Net) - FlowCam, (b) HSN (High-Speed-Net) - ZooScan. More discrete sampling, focus around islands: (c) Bongo**
 214 **Net - FlowCam and (d) Manta - ZooScan (plankton and plastic samples). Island stations, station within 200 nautical**
 215 **miles of an island, are represented inside a yellow circle. The 'not yet analysed' stations in the figure legend mean that**
 216 **the samples have not yet been scanned for the ZooScan dataset and have not been taxonomically validated for the**
 217 **FlowCam dataset.**

218



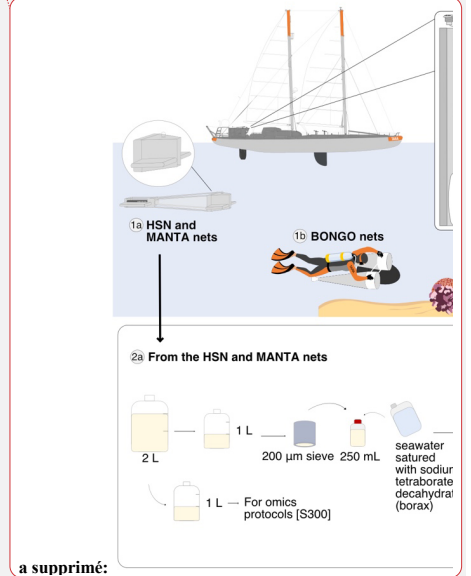
219

220 Figure 3. Schematic overview of the sampling events and protocols used during the Tara Pacific expedition for
 221 quantitative imaging. The top left panel corresponds to the sampling events with the deployed plankton nets: (1a) the
 222 330 µm High Speed Net (HSN) and the 333 µm Manta net, (1b) the 20 µm Bongo nets attached to the underwater
 223 scooter and (1c) the 20 µm Deck Net (DN) on the deck of the Tara. Samples from DN (2c) and Bongo (2b) were imaged
 224 live with the FlowCam (20–200 µm) and samples from HSN and Manta (2a) were imaged with the ZooScan (> 300 µm).
 225 For the ZooScan analysis, samples were fixed using formaldehyde and stored on board and analysed on the Imaging
 226 Quantitative Platform (PIQv) in the laboratory in Villefranche-sur-Mer, the protocols in this platform are detailed in
 227 the section: "On the PIQv lab" (3a). **Somes drawings were taken from Lombard et al. 2023 modified (credit N. Le**
 228 **Bescot).**

229 2.1.1 Deck-Net sampling

230 Surface water samples were collected using a custom-built water pumping system named "Dolphin". It consists
 231 of a stainless-steel pyramidal frame with a front aperture of 0.04 m wide and 0.40 m high, deployed from the
 232 starboard **side** of the ship (see pictures in Gorsky et al., 2019). The Dolphin was used underway while sailing and
 233 was connected to a peristaltic pump (max flow rate = $3 \text{ m}^3 \text{ h}^{-1}$) mounted on the deck of the schooner Tara. The
 234 system was equipped with a flowmeter to record flow rates. The pumped water was filtered through a 20 µm net
 235 (Deck-Net) that was mounted on the wall of the wet lab (Fig. 3; 1c and pictures in Gorsky et al., 2019). Before
 236 entering the Deck-Net, the pumped water passes through a 2000 µm mesh filter. Deck-Net pumping lasted 1 to 2
 237 hours, depending on plankton concentration. Samples were divided into subsamples, which included one
 238 subsample for quantitative micro-plankton imaging analysis on live samples (LIVE20; Fig. 3; 2c) and the
 239 remaining for specific protocols detailed in Lombard et al. (2023). Further information on the Dolphin system,
 240 the Deck-Net, and various protocols based on this sampling can be found in Gorsky et al. (2019) and Lombard et
 241 al. (2023).

a supprimé :
 a supprimé: the
 a mis en forme : Légende
 a supprimé: -
 a supprimé: ,
 a supprimé: the
 a supprimé: -
 a supprimé: , (c) the HSN (High-Speed-Net) - ZooScan
 a supprimé: the
 a supprimé: ¶



a supprimé:
 a supprimé: All sample references are defined in Lombard et al. 2023 (i.e. [S20], [E20], [H20], etc.).

254 **2.1.2 Bongo nets sampling**

255 Plankton larger than 20 μm were sampled at ~ 2 m below the sea surface using two small diameter Bongo plankton
256 nets with 20 μm mesh size and an opening area of 0.071 m^2 . ~~These nets were towed by divers using underwater~~
257 ~~scooters~~ (Fig. 3; 1b) and towed for about 15 min at maximum speed ($0.69 \pm 0.04 \text{ m s}^{-1}$). Each net was equipped
258 with a flowmeter rated to provide accurate measurements at speeds above 0.3 m s^{-1} , but, the relatively low
259 maximum speed of the underwater scooter was insufficient to allow seawater to flow through the 20 μm mesh fast
260 enough to trigger the rotation of the flowmeter. Therefore, volume was estimated from the tow speed and tow
261 duration using the following Eq. (1):

262 Bongo volume = $0.071 \times \text{tow speed} \times \text{tow duration}$ (1)

263 **2.1.3 HSN and Manta nets sampling**

264 Simultaneously with the deployment of the Dolphin to collect microplankton, the High Speed Net (HSN) was
265 towed to sample the mesoplankton. The HSN was equipped with a 330 μm mesh and designed to be deployed
266 while sailing up to 9 knots (average speed deployment: 6.7 knots). The HSN features the same mouth opening as
267 the Dolphin system, consisting of a stainless-steel pyramidal frame with a front aperture measuring $0.40 \times 0.04 \text{ m}$
268 (see zoom on the HSN mouth system on Fig. 3). The base opening of this pyramidal structure measures $0.34 \times$
269 0.34 m . This net was deployed from the starboard ~~side~~ and towed at a distance of 50–60 m behind the ship (to
270 avoid it being in the wake of the ship), for a period of 60–90 min (depending on plankton density). In addition to
271 the HSN, Manta net was also deployed in some locations (Fig. 2). The Manta net have rectangular frame of
272 $0.16 \times 0.60 \text{ m}$ mouth opening with a 4 m long net with 333 μm mesh size, and was used at a maximum speed of 3
273 knots, for an average of 30–40 minutes.

274
275 Flowmeters were mounted at half of the opening height above the bottom of the opening on both HSN and Manta
276 nets to ensure it was well submerged during deployment while measuring the filtered volume. Theoretical volumes
277 were calculated taking into account a 3/4 mouth opening of the HSN and Manta nets, 0.3×0.04 and 0.6×0.12
278 m, respectively (see Eq. (3), (4) and (5)). As these nets are surface nets, the water collected actually passed through
279 $\sim 3/4$ of the opening height (see photos of deployments in Gorsky et al., 2019). To calculate volumes from the
280 flowmeter for the HSN, we considered an opening of $0.34 \times 0.34 \text{ m}$, corresponding to the dimensions of the
281 pyramid base opening where the flowmeter was positioned inside the HSN (Eq. (2)). We compared the volume
282 estimated from the flowmeter readings with theoretical estimation using the towing distances. We computed the
283 towing distances using the minute binned latitude and longitude recorded with the Tara's GPS along each
284 deployment. We calculated the distance between the start-end latitude and start-end longitude for each minute, to
285 calculate the distance per minute covered by the boat. We then summed these 'per-minute' distances over the
286 duration of the deployment to obtain a calculated distance that is as close as possible to the true towing distance
287 and accounts for potential modification of the boat's heading during deployments. The equations for calculating
288 the filtered volumes are therefore as follows. ~~The 0.3 factor in the flowmeter volume equation corresponds to the~~
289 ~~impeller pitch, as recommended by Hydrobios, to convert the number of revolutions into towing distance.~~

290 HSN flowmeter volume = flowmeter end – flowmeter start $\times 0.3 \times$ (HSN mouth opening area) (2)

291 HSN theoretical volume = tow distance \times (HSN mouth opening area) (3)

292 Manta flowmeter volume = flowmeter end – flowmeter start $\times 0.3 \times$ (Manta mouth opening area)
293 (4)

294 Manta theoretical volume = tow distance \times (Manta mouth opening area) (5)

295 Simplified Metadata in csv provides both flowmeters and theoretical volumes for HSN and Manta net, enabling
296 the user to select the filtered volume for the calculation of quantitative descriptors. A discussion of the biases
297 associated with each estimate is given in section 3.2. The filtered volumes uploaded as metadata in EcoTaxa
298 (EcoTaxa export table in tsv, see part 2.5) and used to compute quantitative descriptors (see part 2.5) are the
299 theoretical volumes calculated from the distance (see the results of technical validation part 3.2.1).

a supprimé: ,

a supprimé: attached to an underwater scooter

a supprimé: see

a supprimé: :

a supprimé: 0.34×0.34

a supprimé: \rightarrow

a supprimé: 0.3×0.04

a supprimé: \rightarrow

a supprimé: 0.6×0.12

a supprimé: $\rightarrow \rightarrow$

a supprimé: 0.6×0.12

a supprimé: $\rightarrow \rightarrow$

312
313 Once recovered, samples collected both by the HSN net and the Manta net followed the same procedure (Fig. 3;
314 2a). The sample was divided into two 1 L fractions (details in Gorsky et al., 2019). One fraction was concentrated
315 on a 200 µm sieve and resuspended in a 250 mL double-sealed bottle using filtered seawater saturated with sodium
316 tetraborate decahydrate (borax), fixed with 30 mL of 37% formalin solution and stored at room temperature for
317 taxonomic and morphological analysis by imaging methods in the laboratory (samples named [F300]). The other
318 fraction was used for omic analysis.

319 2.2 Acquisition and treatment of plankton imaging data

320 Sample labels were annotated by different users at different times during the expedition and are therefore not
321 homogeneous. In order to avoid confusion or misunderstanding of the labelling of the samples, an additional
322 column has been created in the csv Simplified Metadata (column "Homogenous sample names") with
323 homogeneous names for all datasets.

324 2.2.1 FlowCam analysis

325 Samples from the Deck-Net (250 mL) and Bongo net (50mL) were imaged live directly on board using a FlowCam
326 Benchtop B2 series (Fluid Imaging Technologies; Sieracki et al., 1998) equipped with a ×4 objective and a 300
327 µm deep glass flow cell to examine the micro-plankton samples (size range 20-200 µm: Fig. 3; 2c). Each sample
328 was first passed through a 200 µm sieve to remove large objects that could clog the FlowCam imaging cell.
329 Samples were then diluted or concentrated to achieve optimum object flow. The auto-image mode was used to
330 image the particles in the focal plane at a constant flow rate.

331 2.2.2 ZooScan analysis

332 The ZooScan imaging instrument (Gorsky et al. 2010) was used to study the mesoplankton. Samples collected
333 from the HSN and Manta nets ([F300]) were imaged at the Quantitative Imaging Platform (PIQv) of the Institut
334 de la Mer de Villefranche (Fig. 3; 3a). In addition, preserved zooplankton samples are stored in the Collection
335 Center for Plankton of Villefranche (CCPv). The formaldehyde solution was replaced by filtered seawater during
336 the analysis.

337

338 *Plankton samples analysis from HSN and Manta nets on the ZooScan*

339

340 Before scanning on the ZooScan, plankton samples were divided using a Motoda splitter (Motoda, 1959) to obtain
341 a concentration of approximately between 1000 and 2500 objects per subsample and scanned with the ZooScan.
342 This sampling strategy correctly accounted for the many small organisms as well as the large ones that might be
343 under-sampled when subsampling with the Motoda box. This limit ([1000- 2500] objects) was defined by the
344 PIQv platform to avoid the overlap of planktonic organisms, while retaining enough organisms to give a reliable
345 quantitative measurement of the sample. After each scan, a quality control was systematically carried out
346 concerning i) the quality of the scanned image and ii) the number of objects imaged, to ensure that that the number
347 of objects is within the limits given above. The quality control tool for imaging data is accessible on the PIQv
348 website: <https://sites.google.com/view/piqv/>. After treatment in the ZooScan, all samples were re-concentrated on
349 a 200 µm sieve and resuspended in a 250 mL double-sealed bottle using filtered seawater saturated with borax,
350 fixed with 30 mL of 37% formalin solution and returned to the CCPv.

351

352 The borax (sodium tetraborate decahydrate) used as a buffer may form crystals grains, forming white crystals. If
353 the borax solution was not filtered sufficiently, crystals would end up in the plankton samples, be digitised and
354 counted as objects. Thus, if Borax was not filtered sufficiently, white crystals may represent a large proportion of
355 the objects within the 1000-2500 limit and thus bias the quantitative measurement of the plankton. We identified
356 24 samples containing borax crystals during the analysis. Therefore, prior to scanning, these samples were
357 thoroughly rinsed with filtered seawater through a 300 µm mesh sieve to remove a maximum of borax crystals

a supprimé: has a tendency to crystallise

a supprimé: could

360 from the sample. A 200 µm mesh sieve was placed below the 300 µm sieve in order to conserve the initial sample
361 in the collection (CCPv). Analysis on the ZooScan was performed from the 300 µm sieve.

362 *Plastic sampling from Manta net*

363
364
365 Samples from the Manta nets were gently transferred to a Petri dish. Plastic-like particles were manually separated
366 from other components such as wood, zooplankton, and organic tissues (Fig. 3; 3a). Entangled pieces of plastic
367 were picked up manually from zooplankton and aggregated under a stereoscopic dissecting microscope, using
368 forceps. The visual criteria used to classify a microfiber as synthetic were the absence of cellular structures and
369 scales on the surface, a curved shape with a uniform surface, a uniform thickness along the entire length of the
370 filament, spots, and strong strands (Barrows et al., 2018; Hidalgo-Ruz et al., 2018). Each sample was examined
371 twice to ensure the detection of most of the plastic particles. Isolated plastic particles were then imaged with
372 Zooscan. To minimise the plastic contamination of the samples, a quality control approach was undertaken
373 following the protocol described by Pedrotti et al. (2022).

374 **2.3 Images processing**

375 For FlowCam and ZooScan, the full methodology used can be found in their respective manuals
376 (<https://sites.google.com/view/piqv/piqvmanuals/instruments-manuals>; for the ZooScan the protocol is also
377 available on zenodo by Jalabert, 2022). Images generated by FlowCam and ZooScan were processed using the
378 ZooProcess software in ImageJ (Gorsky et al. 2010) which extracts segmented objects as vignettes. During this
379 process, each vignette was associated with a set of 46 morphometric measurements for object characterization,
380 including grey levels, fractal dimension, shape and size, which were imported into the EcoTaxa web application
381 (Picheral et al. 2017) for taxonomic classification. For ZooScan, the ZooProcess software includes a tool that
382 enables the digital separation of potentially touching or overlapping objects in the original image. If two objects
383 (possibly two plankton organisms) are touching, they will be considered as a single vignette and assigned a single
384 label, which could therefore bias estimates of abundance and size, as described in Vandromme et al. (2012).
385 Objects that were still touching after the application of the ZooProcess automatic tool were identified and
386 separated using the ZooProcess manual separation tool to improve the quality of the subsequent taxonomic
387 annotation, counts and size structure analysis of the zooplankton. For each ZooScan dataset, this quality control
388 step was systematically performed during taxonomic annotation.

389 **2.4 Taxonomic identification**

390 Using image recognition algorithms on EcoTaxa, predicted taxonomic categories were validated or corrected by
391 trained taxonomists. For the majority, the taxonomic classification effort was possible up to the genus and only in
392 rare cases up to the species. A number of organisms could not be reliably taxonomically identified due to a lack
393 of identification criteria and were therefore grouped into temporary categories (t00x) following similar
394 morphological criteria. Nine different trained taxonomists from the PIQv platform annotated FlowCam and
395 ZooScan vignettes on these datasets. Annotations of FlowCam and ZooScan vignettes from the different nets were
396 also done by different taxonomists but the list and the global criteria to identify a group were common. To reduce
397 operator bias between taxonomists and to ensure taxonomic consistency, a final stage of homogenisation was
398 carried out by two taxonomists after all vignettes had been validated. At the time of publication of these datasets,
399 copepod genera had not been homogenised for ZooScan, but homogenisation will be pursued in the future and the
400 published SEANO dataset will be updated accordingly. Overall, these datasets are published on the SEANO
401 flexible platform that allows updates and corrections, so that taxonomic annotations can be improved over time.
402 All vignettes with taxonomic annotations are visible on the open access project in EcoTaxa (section 4).

403 **2.5 Case of FlowCam taxonomic identification for objects smaller than 45 µm**

404
405
406 The Tara Pacific settings for the FlowCam live analysis generates many more images than the ZooScan. For
407 example, for station oa140, the ZooScan counts 1 435 images compared to 42 915 images for the FlowCam. Given

a supprimé: For ZooScan, ZooProcess includes a tool that allows for the digital separation of possible touching objects in the original image. As touching objects can affect estimates of abundance and size (Vandromme et al. 2012).

a supprimé: Remaining touching objects after the application of the tool were identified for in all vignettes and objects were separated using the ZooProcess separation tool to improve the quality of further taxonomic annotation, counts and size structure analysis of zooplankton. A quality control step on the number of remaining multiples was systematically performed after the taxonomic annotation.

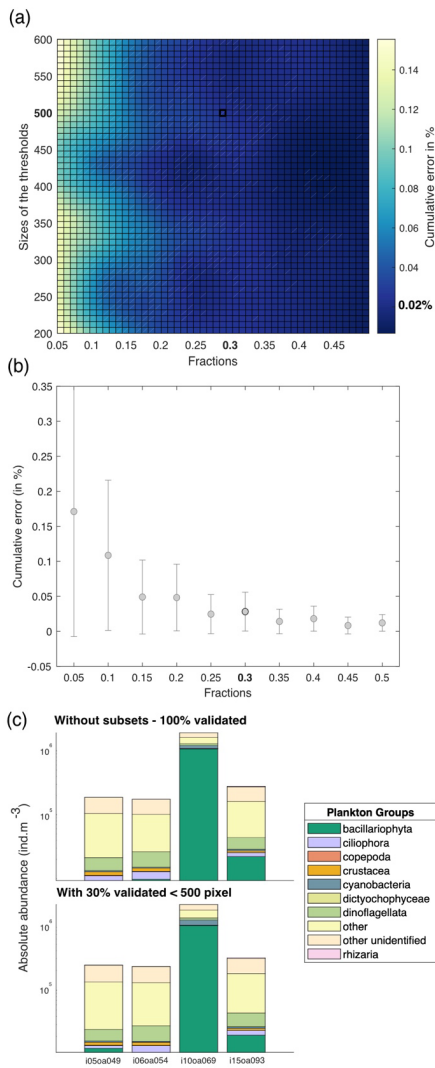
a déplacé (et inséré) [1]

a déplacé vers le haut [1]: Annotations of FlowCam and ZooScan vignettes from the different nets were also done by different taxonomists but the list and the global criteria to identify a group were common.

423 that taxonomists annotated images on an image-by-image basis, the validation or correction of the automatic
424 classification on these numerous FlowCam images would require a much higher investment of time than for the
425 ZooScan samples. In addition, the resolution of the FlowCam images of the smallest organisms does not allow us
426 to classify them properly and at a sufficient precision. Therefore, we validated only 30% of the total images
427 smaller than 500 pixels (equivalent to ~45 μm in ESD), randomly picked, assuming that this 30% random
428 subsample leaves a statistical count that is sufficiently representative of the population. Prior to this choice, a
429 series of tests were conducted to assess the impact of different fraction of image validation at varying object size
430 thresholds. Samples were randomly selected and 100% of the images were taxonomically validated. Subsequently,
431 a series of simulations (three times for the four samples, random sampling each time) were conducted to assess
432 the impact of varying size thresholds (i.e. from 200 to 600 pixels, equivalent to 18 to 55 μm , with a step of 50
433 pixels) on the proportion of total images to be annotated (fractions from 5% to 50%, with increments of 5%). We
434 compared the results of these simulations by using the relative Root Mean Square Error (RMSE). The RMSE
435 values were divided by the total number of 100% validated values and multiplied by 100 to express the cumulative
436 error as a percentage. Results are shown in Fig. 4 and illustrate the cumulative error across the absolute abundance
437 values. For our chosen threshold of 500 pixels and subsets at 30% (highlighted in bold on the Fig. 4), we observed
438 induced errors of 0.02%. In Figure 3d, we present the absolute abundance and taxonomic group composition of
439 plankton from the four samples that were 100% taxonomically annotated, alongside the same four samples that
440 were only 30% (< 500 pixels) annotated. These samples show highly comparable results in both absolute
441 abundance and taxonomic composition (data not shown). We carried out the same analysis as described in Figure
442 4 for the total size spectrum, **slope of the NBSS**, and **for the taxonomic composition** (relative abundance). They
443 showed an induced error of 20% and 12%, respectively. **This supplementary analysis can be found in appendix C.**
444 The software ZooProcess 8.27, available on the PIQv website, now includes the capability for subsampling on
445 Flowcam data.

a supprimé: (

a supprimé:)



448
449

450 **Figure 4. (a)** Estimated cumulative error associated with partial validation of particles below a size cut-off threshold
 451 ranging from 200 to 600 pixels and validated fractions ranging from 5% to 50%. Errors are computed as the percentage
 452 Root Mean Squared Error (RMSE) between fully validated samples and partially validated samples in three different
 453 metrics for cumulative error in absolute abundance. RMSE values represent the outcomes of simulations, each
 454 conducted three times for the four samples, with random sampling. (b) Cumulative error according to the Fractions
 455 chosen. The threshold is fixed at 500 pixels. (c) Comparison between the absolute abundance (ind.m⁻³) and plankton
 456 group composition for samples taxonomically annotated at 100% and for the same samples annotated at 30% below
 457 the threshold of 500 pixels, equivalent to 45 μ m.

458 **2.5 Datasets**

459 **2.5.1 Plankton images on EcoTaxa and the associated tsv.**

460 The datasets include 4 datasets of microplankton imaged by the FlowCam and sampled by the Deck-Net and the
 461 Bongo Nets, and mesoplankton imaged by the ZooScan sampled by the HSN and the Manta. All of the sorted
 462 images of plankton, plastic and particles are visible on the open-access projects on the EcoTaxa web application.
 463 The *.tsv files exported from the EcoTaxa platform are provided. Readme tables for FlowCam and ZooScan *.tsv
 464 are also provided to facilitate their use.

a supprimé: This paper presents the quantitative imaging datasets collected during the Tara Pacific Expedition.

465 **2.5.2 Quantitative descriptors to study the micro- and meso-plankton community**

466 For each dataset, we designed a table combining the metadata and data from which we have calculated quantitative
 467 descriptors of planktonic communities: abundance (ind/m³), biovolume (mm³/m³; proxy of biomass) and Shannon
 468 diversity Index. Abundance (ind/m³) and biovolume (mm³/m³) were calculated taking into account the volume of
 469 water filtered by the plankton samplers (see formula in Table 1). Biovolumes (in mm³/m³) were computed using
 470 area, riddled area, and ellipsoidal measurement of each object, and are available in the *.csv table (following
 471 Vandromme et al., 2012; formula in Table 1). For analysis shown here, major and minor axes of the best ellipsoidal
 472 approximation were used to estimate the biovolume of each object, following the recommendations of
 473 Vandromme et al. (2012). Size was expressed as equivalent spherical diameter (ESD, μm , see formula Table 1).
 474 Diversity was calculated using the Shannon index (H: see formula Table 2). It is important to note that Shannon's
 475 diversity index is dependent on the number of taxonomic categories, as defined by Shannon and Weaver (1949),
 476 it assumes that individuals are randomly sampled from an independent large population and that all species are
 477 represented in the sample. However, in the majority of cases, taxonomic classification was possible up to genus
 478 level using quantitative imaging methods. This must be taken into account in these Shannon diversity indices,
 479 which therefore differ from more commonly used taxonomic categories. The individual biovolumes of the
 480 organisms were arranged in Normalised Biomass Size Spectra (NBSS), as described by Platt & Denman (1978),
 481 along a harmonic range of biovolumes such that the minimum and maximum biovolumes of each class are linked
 482 by: $B_{vmax} = 20.25 B_{vmin}$. The NBSS was obtained by dividing the total biovolume of each size class by its biovolume
 483 interval ($B_{vrange} = B_{vmax} - B_{vmin}$). The NBSS was representative of the number of organisms (abundance within a
 484 factor) per size class. This can provide insight into ecosystem structure and function through the 'size spectrum'
 485 approach, which generalises Elton's pyramid of numbers (Elton, 1927, Sheldon, 1972, Trebilco et al., 2013). The
 486 NBSS size spectra of each sample (in abundance/ μm) is provided in a separated zip files (.csv). Plankton
 487 abundance and biovolume were calculated for each taxonomic annotation and for different levels of grouping:
 488 living or nonliving, plankton groups and trophic association. The full list of these groups linked to all EcoTaxa
 489 taxonomic annotations is given in the Table A1 to A4 (appendix A) of the taxonomic list and groups in each
 490 dataset.

a supprimé: . Tables

Descriptors		Formulas for FlowCam	Formulas for ZooScan
Abundance (ind/m ³): Number of individus in the sampling/ m ³		$(\text{object_annotation_category} \times \text{sample_conc_vol_ml}) / (\text{acq_fluid_volume_imaged} \times \text{sample_initial_col_vol_m3})$	$(\text{object_annotation_category} \times \text{acq_sub_part}) / \text{sample_tot_vol}$
Biovolume (m ³ / m ³): Volume biomass of individus in the	Plain biovolume	$(4/3 \times \prod x (\sqrt{(\text{object_area}) / \prod})^3 \times \text{sample_conc_vol_ml}) / (\text{acq_fluid_volume_imaged} \times \text{sample_initial_col_vol_m3})$	$((4/3 \times \prod x (\sqrt{(\text{object_area}) / \prod})^3) \times \text{acq_sub_part}) / \text{sample_tot_vol}$

sampling/ m ³	Riddled biovolume	$(4/3 \times \pi \times (\sqrt{\text{object_area_exc}} \text{ (mm}^2) / \pi))^3 \times \text{sample_conc_vol_ml} / (\text{acq_fluid_volume_imaged} \times \text{sample_initial_col_vol_m3})$	$((4/3 \times \pi \times (\sqrt{\text{object_area_exc}} / \pi))^3) \times \text{acq_sub_part} / \text{sample_tot_vol}$
	Ellipsoid biovolume	$(4/3 \times \pi \times [(\text{object_major}/2) \times (\text{object_minor}/2)] \times \text{sample_conc_vol_ml} / (\text{acq_fluid_volume_imaged} \times \text{sample_comment_or_volume}))$	$((4/3 \times \pi \times [(\text{object_major} \text{ (mm)}/2) \times (\text{object_minor} \text{ (mm)}/2)] \times \text{acq_sub_part}) / \text{sample_tot_vol}$
Diversity Shannon Indice (H)		$-\sum (\text{abundance relative (\%)} / 100) * \log(\text{abundance relative (\%)} / 100)$	
Equivalent Spherical Diameter (ESD, μm)		$2 \times \sqrt{(\text{object_area} \times \text{process_pixel}^2 / \pi)}$	
<p>Data description</p> <p>object_area : surface area of the object [pixel²] object_area_exc : surface area of the object excluding holes (object_area*(1-(object_%area/100)) [pixel²] object_minor : length of secondary axis of the best fitting ellipse for the object [pixel] object_major : length of the primary axis of the best fitting ellipse for the object [pixel] process_pixel : dimension of the side of a pixel in the scanned image [mm]</p> <p>Data description for FlowCam See Export EcoTaxa FlowCam read me.csv</p> <p>object_annotation_category : taxon display_name in Ecotaxa sample_conc_vol_ml : concentrated or diluted water volume (from sample_comment_or_volume) [mL] acq_fluid_volume_imaged : flowcam total images volume [mL] sample_initial_col_vol_m3 : initial collected volume, (if nets : sum of the nets) [mL]</p> <p>Data description for ZooScan See Export EcoTaxa ZooScan read me.csv</p> <p>object_annotation_category : taxon display_name in Ecotaxa acq_sub_part : subsampling division factor of the sieved fraction of the sample sample_tot_vol : total filtered volume by the sampling gear [m3]</p>			

a mis en forme : Exposant

a mis en forme : Police :Non Gras

a mis en forme : Police :Non Gras

a mis en forme : Police :Non Gras, Non Italique

495
496 **Table 1. Formulas used to calculate quantitative variables in datasets. The variable names correspond to the real names**
497 **of the variables in the exports (tsv files) and are described in the table.**

498 **3. Technical validation and discussion**

499 **3.1 Limitations of Bongo net micro-plankton sampling for quantitative estimations**

500 Both the Bongo nets and the Deck Net consisted of a 20 μm mesh to collect surface micro-plankton throughout
501 the expedition. A key difference between these two nets lies in their deployment locations, which correspond to

distinct environments: Bongo nets were deployed near islands, reefs, or within lagoons, while the Deck Net was deployed in the open ocean. These environments are characterized by differing chlorophyll a concentration, with a clear increase observed near islands and within lagoons, as highlighted in Bourdin et al. (2024). As such, we expected higher plankton concentrations in the reef and lagoon areas, and consequently, in the Bongo net samples. However, the majority of Bongo net samples showed lower concentrations than nearby open ocean samples from the Deck Net, as evidenced by the NBSS size spectra (Fig. 5a).

This discrepancy raises concerns about our reliability of the volume-filtered estimates, whether based on flowmeters or theoretical calculations, which are critical for consistent quantitative plankton sampling. Regarding the flowmeters, as mentioned in the methods section, Bongo nets were equipped with flowmeters rated for speeds above $0.3 \text{ m}\cdot\text{s}^{-1}$. However, the relatively low towing speed of the underwater scooter was insufficient to generate enough water flow through the $20 \text{ }\mu\text{m}$ mesh to rotate the flowmeters reliably. For the theoretical volume, the deployment time of the Bongo nets by divers was highly uncertain. The uncertainty surrounding the theoretical volume stemmed from inconsistent deployment times recorded by the divers and methodological biases associated with using an underwater scooter, which made the filtered volume estimates unreliable. Moreover, the suspended particle concentrations were very variable for different sampling sites which complicated the correct prediction of the towing time required to obtain reasonable concentrate in the net and avoid clogging.

Overall, the lack of correlation of total chlorophyll a and total phytoplankton biovolume from FlowCam, as shown in figure 5b, indicates that the Bongo net sampling was not quantitative. The chlorophyll a (chl a) values obtained from the HPLC measurements do not represent the same size classes of phytoplankton as those observed with the FlowCam, but we were interested in whether or not there were likely to be similar trends in phytoplankton biomass changes measured for the same station (Fig. 5b). The correlation between chlorophyll a and total phytoplankton biovolume of the Bongo being lower than for the Deck-Net samples. This suggests that phytoplankton biovolume was underestimated relative to chlorophyll a in the Bongo samples. Given the methodological limitations of the Bongo net filtration volume estimation, our most plausible hypothesis is an overestimation of the theoretical volume likely due to clogging. Therefore, as a conclusion, it is highly recommended to use Bongo net samples for qualitative analysis only.

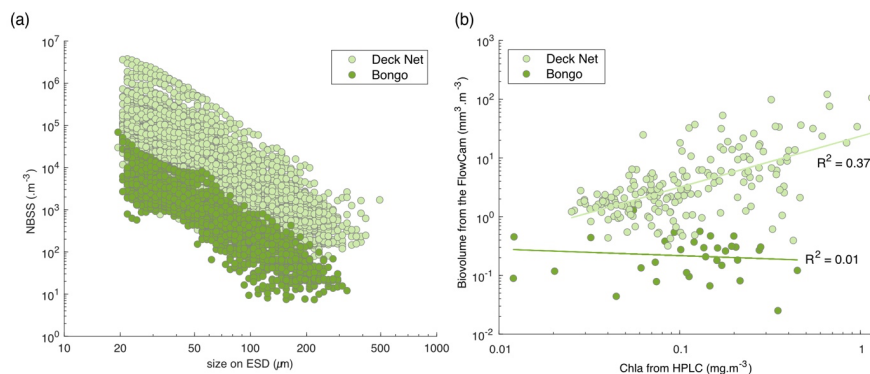


Figure 5. (a) Comparison of Normalised Biovolume Size Spectra (NBSS; in log-log) of the live plankton between the Bongo nets (34 samples) and the Deck Net (207 samples). (b) Phytoplankton biovolume ($\text{mm}^3\cdot\text{m}^{-3}$) estimated from the FlowCam samples, which were collected using the Bongo nets and the Deck Net, according to the Chla values obtained from the HPLC measurements at the same station. The selection of phytoplankton organisms was made possible by taxonomic validation of FlowCam images from these two nets.

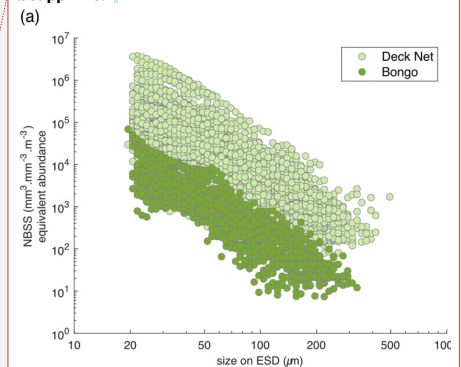
a supprimé: The Bongo was deployed on the reef or in the lagoon while the Deck Net was deployed in the open ocean. Although we expect plankton concentration on the reef and in the lagoon, man

a supprimé: y

a supprimé: This underestimation of concentration may suggest an overestimation of the volume of Bongo filtered.

a supprimé: Similar trends appear to be found for the Deck Net samples, while there is a lack of similar trends for the Bongo. The divers were fully submerged in the water, so we assume that the current speed should have had little or no effect on the theoretical volume estimation. Uncertainty may be associated with the recording of tow duration (maximum 15 minutes), too long for these net characteristics and such suspended matter concentrations, which would lead to clogging of the nets. The Bongo nets have a mesh size of $20 \text{ }\mu\text{m}$, an opening area of 0.071 m^2 and an average filtered volume of $\sim 100 \text{ m}^3$. Indeed, calculations from Smith et al. (1968a) give an average ratio of filtration efficiency (filtered area divided by the mouth area) of ~ 1380 , a value identified by these authors as susceptible to clogging. Therefore, it is strongly recommended quantitative imaging Bongo net samples are only used for qualitative purposes or semi-quantitative analysis.

a supprimé: ¶



a supprimé: ind

a mis en forme : Exposit

564 3.2 Benefits and limitations of high-speed deployment

565 During the Tara Pacific open ocean transects, we decided to take on the challenge of collecting plankton samples
566 while sailing at speeds of up to 9 knots. This high-speed sampling provides valuable opportunities to expand and
567 optimise the coverage of our sampling with a daily frequency. Initially, the Tara Pacific expedition was designed
568 to focus on coral reefs (Planes et al., 2019). The addition of high-speed sampling allowed for the opportunistic
569 use of transit periods, covering a significant spatial area of the expedition. As a result, one of the most valuable
570 aspects of the Tara Pacific plankton samples is the daily collection of samples approximately every 150 to 200
571 nautical miles, covering a wide range of oceanic structures across the Pacific basin. However, it is important to
572 note that, given the patchy spatial distribution of plankton (Robinson et al., 2021), this sampling scale is somehow
573 discrete rather than continuous. This designed sampling is also valuable as we aimed for 'end-to-end' sampling of
574 surface waters (Gorsky et al., 2019) with the micro to macroplankton fractions presented in this article. However,
575 the constraint of surface sampling and of deploying and retrieving the instruments at cruising speed forced us to
576 develop new robust, relatively small and user-friendly devices adapted for the Tara schooner. The combined
577 deployment of the Dolphin system and the High-Speed Net (HSN) designed to this purpose and present in this
578 article, represents, to our knowledge, the first system enabling discrete sampling of the entire surface planktonic
579 ecosystem with deployment and retrieval at cruising speeds < 9 knots.

a supprimé: strategy

a supprimé: .

a supprimé: approach

a supprimé: particularly

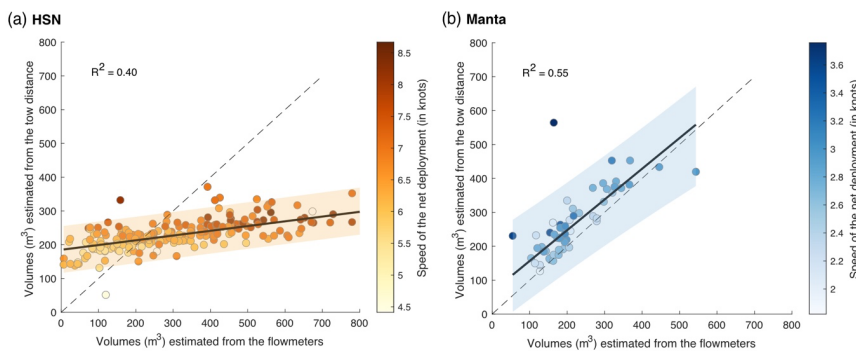
581 The development of the high-speed plankton samplers began in the early 20th century with the well-known
582 Continuous Plankton Recorder (CPR), developed by Alister Hardy in 1926, which is designed to be towed under
583 the surface over long distances at speeds up to 25 knots. Following the CPR, other high-speed net systems
584 emerged, including the Longhurst-Hardy Plankton Recorder (LHPR: Longhurst et al., 1966), Gulf III OCEAN
585 Sampler (Gehring, 1958), and Gulf V plankton sampler (Sameoto et al., 2000) as well as newer low-tech designs
586 (CSN in Von Ammon et al., 2020; Coryphaena in Mériquet et al., 2022). All high-speed zooplankton samplers
587 face the challenge of maintaining filtration efficiency at higher towing speeds. Thus, higher speeds require a larger
588 relative filtration area to optimises filtration efficiency while minimising excessive pressure on the net and
589 mitigating the pressure wave that pushes organisms away from the net (Harris et al., 2000; Keen, 2013; Skjoldal
590 et al., 2013). A critical design principle is therefore to obtain a sufficiently high ratio of mesh filtering area to net
591 opening area (Smith et al., 1968b; Skjoldal et al., 2013). To achieve this, high-speed zooplankton samplers often
592 employ a small initial opening area that widens internally (e.g. CPR has an 1.27 cm² entrance aperture expanding
593 to 5cm x 10cm; the use of conic noses on the Gulf-V and LHPR). This design trade-off essential for pressure
594 reduction, comes at a cost. The small surface area of the mouth opening means a smaller volume filtered, reducing
595 the probability of collecting less abundant, larger organisms (Skjoldal et al., 2013). The avoidance of active
596 swimming zooplankton, net opening area size dependent, is also described as the bias affecting the catch of
597 mesoplankton by Harris et al., 2000. This may be discussed, as increasing tow speed may improve the capture
598 efficiency of zooplankton capable of active avoidance (Skjoldal et al. 2013). Therefore, high-speed sampling
599 methods have the advantages of increasing sampling coverage and frequency, but they also introduce bias due to
600 the pressure generated by high speeds, resulting in even greater undersampling compared to traditional nets (Harris
601 et al., 2000; Cook and Hays, 2001).

602 3.2.1 Impact on filtered volumes estimation

603 One of the primary challenges in quantitative plankton sampling is the estimation of the filtered volume. Because
604 the immersion depth of surface nets changes constantly with waves, wind and boat movement, it is difficult to
605 accurately calculate the volume of water being filtered (reviewed in Pasquier et al., 2022). Results obtained by
606 different studies show that a surface sampling with a difference in immersion depth of a few centimeters can lead
607 to a large difference in the sampled volume (Pasquier et al., 2022). Overall, the impact of high-speed deployment
608 on filtered volume remains largely unexplored in the literature with the exception of Jonas et al (2004). They
609 tested the relationship between CPR filtered volumes estimated by a flowmeter or by theory, and their relationship
610 to CPR deployment speed. Their findings revealed overestimations by the flowmeter compared to theoretical
611 values. This raises concerns about the effectiveness of flowmeters in measuring volumes during high-speed

616 deployments. We therefore investigated whether our high-speed surface sampling approach had an effect on
617 filtered volume measurements.

618
619 For the Deck Net, the water intake was identical in design and mouth opening to HSN but a flowmeter was
620 integrated into the water circuit downstream of the pump as well as two de-bubblers (pictures Fig. 6 in Gorsky et
621 al., 2019). This allowed for reliable estimation of water volumes that were pumped into the Deck-net based on
622 flowmeter recordings (Gorsky et al., 2019). Both HSN and Manta nets were equipped with mechanical flowmeters
623 mounted in the inlet frame, while the towed distance, time and speed were recorded on board to also estimate the
624 theoretical volume filtered. While the HSN was towed between 3.9 and 9 knots, the Manta net was towed at lower
625 speed, between 1.2 knots and maximum speed of 3.6 knots (Fig. 6).
626



627
628
629 **Figure 6. (a) and (b) Linear regression between volumes filtered estimated from the tow distance (theoric volumes; m³)**
630 **and estimated from the flowmeters respectively for the HSN and Manta. The range of 95% confidence intervals is**
631 **represented in orange for the HSN and in blue for the Manta. The 1:1 dotted line represents the linear regression**
632 **obtained if both volumes were similar. The colour of the dots represents the deployment speed of the net in knots.**

633
634 Figure 6 shows a clear discrepancies in the slope of the estimated volumes between the HSN and the Manta,
635 meaning that the theoretical and flowmeter filtered volumes of the Manta are closer to each other than for the
636 HSN. Manta theoretical volumes tend to be higher and thus potentially overestimated compared to flowmeter
637 measurements (Fig. 6b), but the difference remains largely small compared to the HSN. For this one, flowmeter
638 estimation methods provide volumes in the same order of magnitude as the theoretical volume for HSN, yet exhibit
639 considerable differences between stations (mean difference between flowmeter and theoretical volumes per station
640 = 90.5, standard deviation = 172.6; Fig. 6a). Linear regression analysis between this volume differences per station
641 (flowmeters - theoretical volume) and speed deployment showed a significant relationship with a slope coefficient
642 of 91.168 (standard deviation = 11.86, t-test = 7.69 and p-value < 0.001), indicating that higher speeds are
643 associated with greater differences. Consistently with the results of Jonas et al (2004) described before, the high-
644 speed deployment is thus associated with the overestimation of the flowmeters volumes compared to theoretical
645 ones (Fig. 6a). These results indicate that the use of the flowmeters is not appropriate in high-speed conditions.
646 The pressure increase caused by the high speed generates turbulence and could affect the flowmeter rotation and
647 explain the overestimation of the filtered volume for the high-speed that we found. Globally, the turbulence
648 generated could explain the malfunction of flowmeters which are designed and calibrated by the manufactures to
649 accurately measure flow speed in a laminar flow. This result is highlighted by Skjoldal et al. (2019), who assume
650 the use of flowmeters being complex because of their position in relation to the cross-sectional flow field or
651 functioning in a turbulent system.
652

a supprimé :

654 In addition to the speed, we tested the HSN's immersion depth varied when the sea state was high. The HSN was
655 designed to sample the surface ocean, at the air-seawater interface, thus the upper part of its mouth opening was
656 rarely completely submerged during the deployment (see images Fig. 4 in Gorsky et al. 2019). The relationships
657 between wind strength (as a proxy for sea state) recorded by Tara's navigation instruments and the two estimates
658 of HSN sampling volumes showed no correlation ($R^2 = 0.00$ for flowmeter volumes and for theoretical volumes;
659 data not shown). While the flowmeter does not provide accurate flow measurements under turbulent conditions,
660 it appears that the sea state does not affect its volume estimates.

661
662 Therefore, we recommended using the theoretical volume for the HSN. The towing distance used is relative to
663 ground, not to the seawater, therefore there is a potential bias in the theoretical volume estimation due to the non-
664 consideration of the surface current speed. This bias is likely negligible for the majority of our samples located in
665 the subtropical gyres, mostly characterised by relatively low geostrophic currents (Tara Pacific data available
666 Bourdin et al. 2022 in 'at current_speed_copernicus').

667 3.2.2 Quantitative comparison between HSN and Manta

668 The Manta net was designed to study neuston and floating particles, such as microplastics. Thus, it is the most
669 commonly used net for studying surface plankton and widely recognised as a reference system for investigating
670 surface ocean (Eriksen et al., 2018; Karlsson et al., 2020; Pasquier et al., 2022). Both HSN and Manta nets were
671 deployed at the same stations when approaching islands and in the Great Pacific Garbage Patch. The Manta net
672 was deployed in closer proximity to islands than the HSN net. Given that the HSN net was towed for a duration
673 of 60–90 minutes, while the Manta net was towed for approximately 30–40 minutes, the decision was taken to
674 sample with the Manta net in the immediate vicinity of the island, in order to capture the variability associated
675 with the island mass effect.

676
677 We conducted a comparison of the Normalized Biovolume Size Spectra (NBSS; Fig. 7a) obtained from the two
678 nets. The analysis follows the analysis presented in Lombard et al. (2023), incorporating data from 31 additional
679 samples collected by the HSN. The NBSS of both nets was of the same order of magnitude, with Manta
680 biovolumes appearing higher in each NBSS size class (Fig. 7a), suggesting an underestimation by the HSN.
681 Considering the principle that, when represented on a logarithmic scale (as in Fig. 7c), the intercept of NBSS
682 spectra reflects the total abundance of organisms in the studied ecosystem (Platt & Denman, 1978), and assuming
683 the same water masses were sampled, we compared the NBSS intercepts, which support the underestimation by
684 the HSN, as higher intercepts were observed for the Manta (with the NBSS intercept of HSN showing 0.2
685 compared to 0.8 for the Manta). This difference was expected due to the undersampling at high speed compared
686 to traditional plankton sampling discussed above. In contrast to the HSN net, which has a smaller mouth opening
687 leading to a smaller sampling volume, the Manta net benefits from a larger opening and lower towing speed. This
688 combination reduces turbulence and allows for a larger sampling volume, resulting in potentially lower loss. This
689 is reflected in Fig. 7a, where the Manta net captures a wider range of sizes, including larger and rarer fragile
690 organisms. Skjoldal et al. (2019) measured less biomass in the large size fraction and more biomass in the small
691 and medium size fractions at the higher towing speeds. The opposite effect might have been expected for the small
692 fraction due to extrusion (Skjoldal et al., 2019), suggesting that the HSN net may be more effective at capturing
693 smaller organisms. However, this is not clearly demonstrated, as the slopes of the HSN's NBSS are largely
694 equivalent to those of the Manta (mean NBSS slope for HSN = -0.35, std = 0.30 and mean NBSS slope for Manta
695 = -0.30, std = 0.23; Fig. 7a). This also suggests that both nets capture the same trophic plankton ecosystem
696 structure, while the HSN underestimates plankton in each size class.

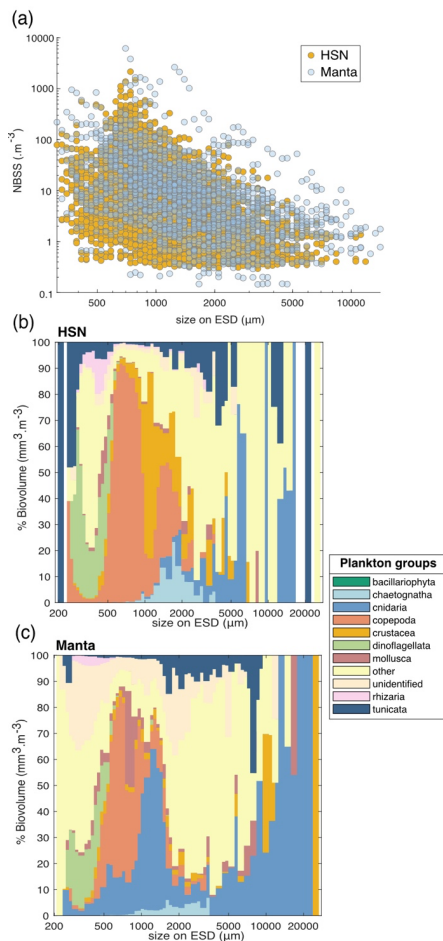
a supprimé: ¶

a supprimé: ,

a supprimé: Abundances based on the

a supprimé: NBSS of both nets were on the same order of magnitude with Manta abundances appearing higher

a supprimé: The opposite effect might have been expected for the small fraction due to extrusion (Skjoldal et al., 2019). Assuming the same water masses were sampled, the HSN net appears to be more effective at capturing smaller organisms, as indicated by the fact that the slopes of the HSN's equivalent abundance is steeper than the Manta's (mean NBSS slope for HSN = -0.35, std = 0.30 and mean NBSS slope for Manta = -0.30, std = 0.23; Fig. 7a).¶

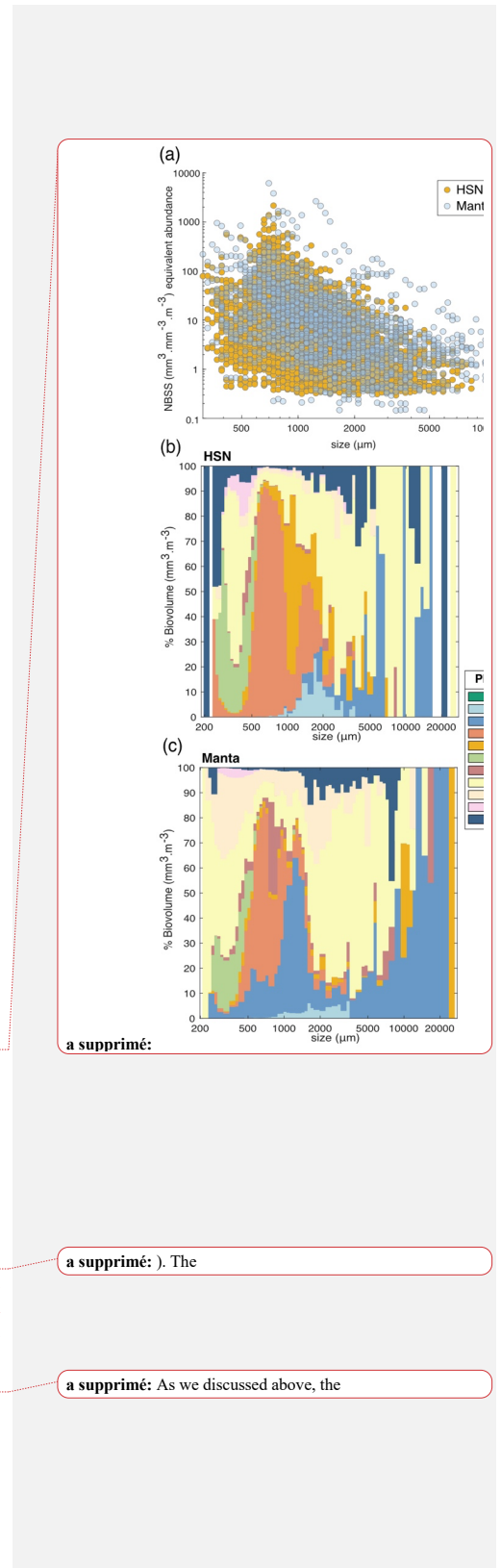


710
711
712
713
714
715

Figure 7. (a) Comparison of Normalized Biovolume Size Spectra (NBSS) of living organisms sampled with HSN in yellow dots and Manta nets in blue dots. Only stations where both were deployed are included in this figure. Average taxonomic composition of the 'plankton groups' in biovolume (mm³·m⁻³) for all stations by size class (in μm) for samples collected with HSN in (b) and Manta net in (c).

716
717
718
719
720
721
722
723
724

All these observed differences may therefore introduce differences in species composition. Investigating the taxonomic composition, the HSN and the Manta show on average relatively similar community compositions (Fig. 7c and 7d; the dinoflagellates are almost entirely composed of the genus *Noctiluca*). Investigating the taxonomic composition in terms of biovolume, the five most represented groups in the Manta dataset are Cnidaria (59%), Copepoda (13%), other (11%), Crustacea (9%), and Mollusca (3%). In contrast, the HSN dataset shows a more even distribution, with other taxa contributing 33%, followed by Cnidaria (28%), Copepoda (19%), Tunicata (10%), and Crustacea (6%). Although there is a general difference in the sampled plankton community, the greatest discrepancies are observed for gelatinous organisms. Thus, HSN net undersampled larger and more fragile



728 organisms such as cnidarians and tunicates (Fig. 7c). This aligns with the limitations of high-speed deployments,
729 which have been shown to damage delicate organisms (Harris et al., 2000; Keen, 2013). This damage to large and
730 fragile plankton could cause the higher concentrations of smaller size classes we found in HSN compared to Manta
731 samples. In contrast, the HSN consistently sampled more robust organisms such as copepods and chaetognaths
732 than the Manta (Fig. 7c and 6d).

a supprimé: like

734 For the quantitative and qualitative comparison of plankton community sampling, we only considered stations
735 where both nets were deployed sequentially (first the Manta, followed by the HSN). Although small, this temporal
736 and spatial difference remains a limitation in our comparison between the two nets. In terms of location, this
737 combination of Manta-HSN deployments was primarily conducted near islands, where plankton concentrations
738 and composition are known to be highly variable (Bourdin et al., 2024; Kristan et al., in prep). Given that the
739 Manta was deployed before the HSN, i.e., closer to the islands, we also expect part of the HSN underestimation
740 signal to be explained by this small spatial difference. Therefore, while our primary hypothesis attributes these
741 differences mainly to the high-speed deployment of the HSN (up to three times greater than that of the Manta),
742 these spatial and temporal factors, in addition to the patchiness distribution of plankton (Robinson et al., 2021),
743 may also play a role in our comparison of the two plankton sampling systems.

a supprimé: Given that plankton concentrations are higher in the areas surrounding the islands (Bourdin et al., in rev) deploying the manta net closer to these islands could also affect the observed differences in plankton concentrations between the two nets.

744 4. General discussion

745
746
747 In conclusion to our investigation of sampling biases associated with the high-speed sampling, the HSN must
748 therefore be considered as semi-quantitative. The use of the HSN introduces an undersampling bias that is also
749 found in other high-speed samplers, as described for the CPR. Nevertheless, we highlight the usefulness of the
750 HSN for sampling surface zooplankton when it is not possible to stop or slow the boat, and its value in extending
751 sampling coverage and frequency. Consistent with the CPR, HSN captures a roughly consistent fraction of the in-
752 situ abundance reflecting the main patterns observed in plankton. Consistent with expected ecological trends,
753 higher plankton abundances and biovolumes are observed in nutrient-rich regions such as coastal and upwellings,
754 whereas oligotrophic gyres exhibit significantly lower biomass (see abundance, biovolume, and diversity maps
755 for each sampling device in appendix B). For example, the trend of increasing plankton abundance due to
756 California upwelling (Checkley and Barth, 2009) appears to emerge regardless of the sampling method used
757 (appendix B: Fig. B1 to B4). Each net is a filter through which we sample the ocean, but if the overall patterns
758 they show are consistent, we can conclude that they are likely to be robust patterns. This is true for many types of
759 sampling nets, as many previous studies have shown (Herdman, 1921; Barnes and Marshall, 1951; Anraku, 1956;
760 Wiebe and Holland, 1968).

761
762 In addition to the unique characteristic of high-speed sampling, these datasets are also distinguished by their focus
763 on surface plankton communities during daytime, offering both advantages and limitations. These surface
764 plankton data enrich interdisciplinary studies of ocean's surface layer, in direct associations with other surface
765 measurements (satellite and atmospheric data; Lombard et al., 2019). This surface ecosystem, hosting a uniquely
766 diverse planktonic community, remains largely unexplored, but appears to play an essential role in ocean-climate
767 feedbacks (Helm, 2021; Hunter, 2023) as a critical interface between atmospheric and oceanic process and
768 contributing significantly to biogeochemical cycles (Falkowski et al., 2008). Processes controlling the abundance
769 and diversity of the surface plankton communities may be significantly different from those in deeper layers
770 (Ibarbalz et al., 2019, Santiago et al., 2023). The surface is also on the frontline of climate change and pollution.
771 Thus, these particular communities face increasing challenges such as rising temperatures, stratification and
772 nutrient stress (Bopp et al., 2013; IPCC, 2022) and floating contaminants ranging from plastics, metals and toxins
773 to petroleum (Helm, 2021). However, surface plankton sampling has limitations regarding the "quantitative
774 representativeness" of the broader plankton ecosystem in the water column. The Tara Pacific sampling was
775 conducted under stable daytime conditions, minimizing variability from diel vertical migration (Lampert, 1989).
776 As a result, zooplankton concentrations do not reflect deeper-dwelling organisms, particularly those migrating to
777 the surface at night, leading to potentially higher abundances within the water column (Lampert, 1989). This is
778 also valuable for phytoplankton communities that are known to be heterogeneously distributed from the surface

785 to deeper waters into the euphotic zone, especially in the transparent oligotrophic waters of the Pacific gyre, where
786 Deep Chlorophyll Maxima can occur tens to hundreds of meters below the surface (Mignot et al., 2014). In terms
787 of comparison with non-surface plankton data, this limitation must be carefully considered by future users.

788 **Conclusion**

789
790
791 The Tara Pacific Expedition is part of the first initiatives aiming to implement a system for discrete sampling of
792 the planktonic ecosystem while operating at cruising speed (5–9 knots), covering viruses to metazoa at the scale
793 of the whole expedition (Gorsky et al., 2019) and focusing on micro- to mesoplankton in this paper. The use of
794 two new sampling systems highlights some biases that lead to undersampling, which is important to consider in
795 subsequent ecological analyses. However, the simultaneous high-speed sampling of the different components of
796 the surface ecosystem may contribute to address the issue of undersampling of the open ocean at difficult-to-reach
797 spatial and temporal scales, a major challenge for marine science. These systems can be improved and adapted to
798 vessels of different sizes and propulsion systems, opening the way to complementary initiatives, such as plankton
799 collection by citizen sailors. (De Vargas et al., 2022; Mériquet et al., 2022).

800
801 In conclusion, using these new sampling methods covering the North and South Pacific and North Atlantic basins,
802 we provide an important dataset focusing on the surface plankton rarely sampled as a whole. Our large-scale
803 analysis reveals an important taxonomic and functional diversity within the surface planktonic communities,
804 encompassing approximately 370 different taxa, primarily identified at the genus level, spanning across 12 major
805 plankton groups and 5 trophic levels. We hope that the dataset presented here, will stimulate further studies (i.e.,
806 biodiversity, biogeochemistry, modeling studies...) using the different environmental imprints recorded during
807 the Tara Pacific expedition (data available in Lombard et al., 2023) to highlight the processes influencing this
808 particular plankton ecosystem, from large scale to mesoscale levels, from taxonomic scale to trophic scale, or
809 from species barcodes to genomes. Such an important dataset will not only serve as a starting point for many
810 studies to deepen our understanding of planktonic ecosystems, their biogeochemical roles, and their socio-
811 economic importance, but could also serve as a reference state of the ecosystem in the context of environmental
812 changes.

813 **4. Data availability**

814 The referenced datasets related to figures are available at:
815 <https://doi.org/10.17882/102537> Mériquet et al., (2024a) (EcoTaxa link: <https://ecotaxa.obs-vlfr.fr/prj/1344>, and
816 <https://ecotaxa.obs-vlfr.fr/prj/1345>),
817 <https://doi.org/10.17882/102336> Mériquet et al., (2024b) (EcoTaxa link: <https://ecotaxa.obs-vlfr.fr/prj/11292>),
818 <https://doi.org/10.17882/102694> Mériquet et al., (2024c) (EcoTaxa link: <https://ecotaxa.obs-vlfr.fr/prj/11370> and
819 <https://ecotaxa.obs-vlfr.fr/prj/11369>)
820 and <https://doi.org/10.17882/102697> Mériquet et al., (2024d) (EcoTaxa link: <https://ecotaxa.obs-vlfr.fr/prj/11353>, and <https://ecotaxa.obs-vlfr.fr/prj/11341>).

821
822
823 The imaging datasets are also summarized in Table 2.

824
825 A key strength of this quantitative imaging dataset is its complementarity with a wide range of environmental data
826 collected during the Tara Pacific expedition. This expedition is described in detail in Lombard et al. (2023), where
827 the full set of environmental datasets is available and referenced: <https://doi.org/10.1038/s41597-022-01757-w>.
828 Environmental data were collected station by station, making it possible to link them directly to our dataset using
829 the station name. Each station is identified by a unique [oa###] code, where the "oa" label is the key identifier for
830 associating environmental measurements with our imaging data. When looking at data at this 'station' level, all
831 environmental data are already compiled and compatible for easy analysis and cross-analysis, and when linked to
832 sample barcodes, they could be further linked to any other associated data (e.g. genomic) by linking them to the
833 sample registry available in Lombard et al 2023, with sample and event registry at:

a supprimé: In conclusion, the use of the HSN introduces an undersampling bias that is also found in other high-speed samplers, as described for the CPR. The HSN must therefore be considered as semi-quantitative. Nevertheless, we highlight the usefulness of the HSN for sampling surface zooplankton when it is not possible to stop or slow the boat, and its value in extending sampling coverage and frequency. Consistent with the CPR conclusion, HSN captures a roughly consistent fraction of the in-situ abundance reflecting the main patterns observed in plankton. For example, the trend of increasing plankton abundance due to Californian upwelling (Checkley and Barth, 2009) appears to emerge regardless of the sampling method used (see Fig. B1 to B4, appendix B). Each net is a filter through which we sample the ocean, but if the overall patterns they show are consistent, we can conclude that they are likely to be robust patterns. This is true for many types of sampling nets, as many previous studies have shown (Herdman, 1921; Barnes and Marshall, 1951; Anraku, 1956; Wiebe and Holland, 1968).

a mis en forme : Police :Gras

a supprimé: The Tara Pacific Expedition introduces, to our knowledge, the first system adapted for discrete sampling of the whole, end-to-end, planktonic ecosystem, from viruses to metazoa, deployed and recovered at cruising speed (5–9 knots). Our observations on these two new sampling systems highlight biases, particularly the under-sampling of fragile organisms (e.g., gelatinous plankton), which is important to consider in subsequent ecological analyses. However, high-speed sampling provides valuable opportunities to expand the coverage and frequency of plankton collection, helping to address the critical issue of under-sampling in the open ocean, a major challenge for global plankton research. This has provided an adaptable framework for studying planktonic ecosystems at spatial and temporal scales that are difficult to achieve. These systems can also be easily adapted to vessels of various sizes and propulsion systems, paving the way for complementary initiatives, such as plankton collection by citizen sailors (De Vargas et al., 2022; Mériquet et al., 2022). ¶

a supprimé: ¶
In conclusion, with these innovative methods, we provide an important dataset covering nearly the whole Pacific Ocean and North Atlantic one, and focusing on the surface plankton which is rarely sampled as a whole, but rather focused on the plastic and large neustonic inhabitants. Such a large dataset, consistently sampled, at a large scale open the way to further studies focusing on how different environmental imprints (Lombard et al., 2023) may affect this particular ecosys (... [2])

a mis en forme : Anglais (G.B.)

a mis en forme : Anglais (G.B.)

a mis en forme : Anglais (G.B.)

Code de champ modifié

a mis en forme : Anglais (G.B.)

a mis en forme : Anglais (E.U.)

a mis en forme : Anglais (E.U.)

Code de champ modifié

a mis en forme : Anglais (E.U.)

a mis en forme : Anglais (E.U.)

900 <https://doi.org/10.1594/PANGAEA.944548>. In addition to station-based data, continuous environmental
 901 measurements from the Tara Pacific expedition (Lombard et al., 2023) can also be linked to our dataset. These
 902 measurements can be linked to plankton net sampling events using date, time and GPS coordinates, all of which
 903 are available in both the plankton and in line environmental datasets. This ensures a robust integration of imaging
 904 and environmental data, facilitating large-scale ecological analyses.

905
 906

a supprimé: The datasets are also summarized in Table 2. ¶

	Datasets			
Name	FlowCam Tara Pacific DN 20 microns	FlowCam Tara Pacific Bongo 20 microns	ZooScan Tara Pacific HSN 330 microns	ZooScan Tara Pacific Manta 333 microns
DOI	10.17882/102697	10.17882/102694	10.17882/102336	10.17882/102537
Sampling Location	Open-ocean and islands sampling	Islands, reef and lagoon sampling	Open-ocean and islands sampling	Open-ocean (Great Pacific Garbage Patch) and islands sampling
Plankton size imaged	(20-200 µm)	(20-200 µm)	(> 300 µm)	(> 300 µm)
Link to open EcoTaxa project	Subset 30% < 500 pixels: https://ecotaxa.obs-vlfr.fr/prj/11353	Subset 30% < 500 pixels: https://ecotaxa.obs-vlfr.fr/prj/11370	https://ecotaxa.obs-vlfr.fr/prj/11292	Subset Plankton images https://ecotaxa.obs-vlfr.fr/prj/1344
	Subset 100 % > 501 pixels: https://ecotaxa.obs-vlfr.fr/prj/11341	Subset 100 % > 501 pixels: https://ecotaxa.obs-vlfr.fr/prj/11369		Subset Plastics images https://ecotaxa.obs-vlfr.fr/prj/1345
	Subset 30% < 500 pixels: Export EcoTaxa FlowCam Tara Pacific DN 20 microns < 500 pixels.zip	Subset 30% < 500 pixels: Export EcoTaxa FlowCam Tara Pacific Bongo 20 microns < 500 pixels.zip		Export EcoTaxa ZooScan Tara Pacific HSN 330 microns.zip
ZIP files with one tsv per samples, raw export from EcoTaxa	Subset 100 % > 501 pixels: Export EcoTaxa FlowCam Tara Pacific DN 20 microns > 501 pixels.zip	Subset 100 % > 501 pixels: Export EcoTaxa FlowCam Tara Pacific Bongo 20 microns > 501 pixels.zip		Subset Plastics images Export EcoTaxa ZooScan Tara Pacific Manta 333 microns plastics.zip

CSV files with ab, bv (x3: area, riddled and ellispoidal), shannon	Descriptors FlowCam Tara Pacific DN 20 microns.csv	Descriptors FlowCam Tara Pacific Bongo 20 microns.csv	Descriptors ZooScan Tara Pacific HSN 330 microns.csv	Descriptors ZooScan Tara Pacific Manta 333 microns.csv
ZIP files with 1 table csv / sample for NBSS (1 NBSS / sample)	NBSS FlowCam Tara Pacific DN 20 microns.zip	NBSS FlowCam Tara Pacific Bongo 20 microns.zip	NBSS ZooScan Tara Pacific HSN 330 microns.zip	NBSS ZooScan Tara Pacific Manta 333 microns.zip

909

910 **Table 2. Summary of data availability, description and useful link for each dataset.**

911 **Appendices**

912

FlowCam Tara Pacific DN 20 microns		
Taxonomic list	Plankton groups	Trophic type
Bacillariophyceae	bacillariophyta	phototroph
Asterionellopsis		
Asterolamprales		
Bacillariaceae		
Climacodium		
Climacodium inter. Crocosphaera		
chainlarge		
chainthin		
multiple < Diatoma		
Pseudo-Nitzschia chain		
Thalassionematales		
Corethron		
Coscinodiscophycidae		
Coscinodiscids		
Bacteriastrum		
Chaetoceros		
Chaetoceros protuberans		
Chaetoceros peruvianus		
Ditylum		
Eucampia		
Hemiaulus		
Fragilariopsis		
Nitzschia		
Planktoniella sol		
Rhizosolenids		

Dactyliosolen		
Guinardia		
Rhizosolenia inter. Richelia		
pennate < Bacillariophyta		
Helicotheca		
Cyanobacteria	cyanobacteria	autotroph
UCYNA like		
cyano a		
cyano b		
Richelia		
attached		
Codonaria	ciliophora	mixotroph
Ciliophora		
Amphorides		
Codonellidae		
Codonellopsis		
Codonellopsis orthoceras		
Cyttarocylis		
Dictyocysta		
Epiplocylis		
Eutintinnus		
Lacrymaria		
Metacylis		
Porococcus		
Rhabdonella		
Rhabdonellopsis		
Salpingella		
Steenstrupiella		
Tintinnida		
Undellidae		
Amplectella		
Xystonellidae		
Dadayiella		
Zoothamniidae		
Dictyochophyceae	dictyochophyceae	phototroph
Gonyaulacales	dinoflagellata	mixotroph
Dinophyceae		
Amphisolenia		
Dinophysis		

Ceratocorys		
Cladopyxis		
Neoceratium		
Neoceratium limulus		
Neoceratium candelabrum		
Neoceratium furca		
Neoceratium fusus		
Neoceratium pentagonum		
Neoceratium geniculatum		
Pyrocystaceae		
Pyrophacus		
Gymnodiniales		
Ornithocercus		
Ornithocercus heteroporus		
Ornithocercus magnificus		
Ornithocercus quadratus		
Ornithocercus steinii		
Oxytoxum		
Phalacroma		
Podolampas		
Protoperidinium		
polar view		
Hemidiscus cuneiformis		
Tunicata	tunicata	grazers
Appendicularia		
Copepoda	copepoda	
Ostracoda	crustacea	
nauplii < Crustacea		
Rotifera	other	omnivorous
trochozoa		
larvae < Annelida		
veliger	mollusca	grazers
Pterosperma	other	phototroph
Rhizaria	rhizaria	mixotroph
Retaria		
Amphibelone		
Acantharia		
Foraminifera		
Nassellaria		

Spumellaria		
cyst	other	-
egg		
egg sac		
multiple < other	-	-
othertocheck	other unidentified	unidentified
darkrods < othertocheck		
lightrods < othertocheck		
othersphere		
t001	other unidentified	unidentified
t003		
t004		
tail < Appendicularia	non-living	-
part < Crustacea		
spines < Acantharea		
part < Ciliophora		
artefact		
badfocus < artefact		
bubble		
detritus		
dark < detritus		
fiber < detritus		
light < detritus		
pollen		
duplicate		
t002		

913
914
915

Table A1. List of EcoTaxa taxonomic annotations and associated groups: plankton groups and trophic type for the FlowCam DN 20 microns dataset.

FlowCam Tara Pacific Bongo 20 microns		
Taxonomic list	Plankton groups	Trophic type
Trichodesmium	cyanobacteria	autotroph
UCYNA like		
Cyanobacteria<Proteobacteria		
Richelia		
Ciliophora	ciliophora	mixotroph

Lacrymaria<Lacrymariidae		
Vorticella		
Codonellidae		
Cyttarocylis		
Epiplocylis		
Dictyocysta		
Metacylis		
Rhabdonella		
Rhabdonellopsis		
Tintinnida		
tintinnid-diatom		
Amphorides<Tintinnidiidae		
Eutintinnus		
Salpingella<Tintinnidiidae		
Steenstrupiella		
Tintinnidae X		
Poroecus		
Undellidae		
Xystonellidae		
part<Ciliophora		
Dinophyceae		
Dinophyceae X		
Amphisolenia		
Ornithocercus		
Ornithocercus magnificus<Ornithocercus		
Ornithocercus steinii		
Phalacroma		
Neoceratium		
Neoceratium candelabrum		
Neoceratium furca<Neoceratium	dinoflagellata	mixotroph
Neoceratium fusus<Neoceratium		
Neoceratium pentagonum		
Cladopyxis		
Ostreopsis		
Pyrocystaceae		
Pyrophacus		
Peridiniales		
Oxytoxum		
Podolampas		
Protoperidinium		

Rhizaria	rhizaria	mixotroph
Retaria		
Acantharea		
spines<Acantharea		
Foraminifera		
Nassellaria<Polycystinea		
Spumellaria		
Radiolaria		
aggregate<Radiolaria		
part<Rhizaria		
spines<Rhizaria		
Bacillariophyceae	bacillariophyta	phototroph
Asterionella		
Coscinodiscophycidae		
Asterolamprales		
Hemidiscus cuneiformis		
Hemidiscus		
Cylindrotheca		
Diatoma		
chainlarge		
chainthin		
multiple<Diatoma		
Licmophora		
Naviculales		
Nitzschia		
Pseudo-nitzschia		
Striatella		
Synedra		
Thalassionematales		
Amphitetras		
Bacteriastrum<Mediophyceae		
Biddulphia		
Chaetoceros<Mediophyceae		
Chaetoceros inter ciliate		
Chaetoceros inter. Calothrix		
Ditylum		
Eucampia		
Hemiaulus		
Odontella sp.		

Odontella<Mediophyceae		
Planktoniella		
Corethron		
Coscinodiscus		
Stephanopyxis		
Rhizosolenids		
Dactyliosolen		
Guinardia		
Rhizosolenia		
Rhizosolenia inter. Richelia		
rhizosolenia inter richelia tmp i		
rhizosolenia tmp i		
centric		
chain<centric		
pennate<Bacillariophyta		
part diatom		
Dictyochophyceae		
Dictyochales	dictyochophyceae	phototroph
Dictyocha		
Annelida		
larvae<Polychaeta	others	grazers
trocophora		
larvae<Annelida		
trochophore		
Copepoda<Maxillopoda		
Calanoida	copepoda	omnivorous
Cyclopoida		
Oithonidae		
Harpacticoida		
Corycaeidae		
Oncaeidae		
part<Copepoda		
nauplii<Crustacea	crustacea	grazers
part<Crustacea		
Bryozoa	other	grazers
trochozoa		

larvae<Echinodermata		
Mollusca	mollusca	
veliger		
larvae<living	other	unidentified
other<living		
egg<other		
egg sac<egg		-
multiple<other	-	-
duplicate		
othertocheck	other unidentified	unidentified
crumple sphere		
darkrods<othertocheck		
lightrods<othertocheck		
t001	other unidentified	unidentified
t002		
t003		
t004		
t005		
t006		
t007		
t008		
t010		
t011		
t012		
t013		
t014		
t015		
t016		
t017		
part<other	non-living	-
part<seaweed		
Micracanthodinium quadrispinum		
artefact		
badfocus<artefact		
bubble		
detritus		

aggregates		
dark<detritus		
fiber<detritus		
light<detritus		
feces		
darkrods<rods		
lightrods<rods		

916

917 **Table A2. List of EcoTaxa taxonomic annotations and associated groups: plankton groups and trophic type for the**
918 **FlowCam Bongo 20 microns dataset.**

ZooScan Tara Pacific HSN 330 microns		
Taxonomic list	Plankton groups	Trophic type
Actinopterygii	other	predators
egg < Actinopterygii		
Annelida	other	omnivorous
Spirorbis		
larvae < Annelida		
Appendicularia	tunicata	grazers
Oikopleuridae		
Bryozoa	other	grazers
cyphonaute		
Chaetognatha	chaetognatha	predators
Hydrozoa	cnidaria	predators
Scyphozoa		
Porpita		
larvae < Porpitiidae		
Siphonophorae		
bract < Abylidae		
gonophore < Abylidae		
nectophore < Abylidae		
Diphyidae		
bract < Diphyidae		
eudoxie < Diphyidae		
gonophore < Diphyidae		
nectophore < Diphyidae		
nectophore < Hippopodiidae		

Abylopsis tetragona		
bract < Abylopsis tetragona		
eudoxie < Abylopsis tetragona		
gonophore < Abylopsis tetragona		
nectophore < Abylopsis tetragona		
bract < Bassia bassensis		
nectophore < Bassia bassensis		
Physonectae		
nectophore < Physonectae		
Velella		
polype < Leptothecata		
polype < Anthozoa		
Cirripedia		
cirrus		
cypris		
nauplii < Cirripedia		
Evadne		
Podon		
Calanoida		
Acartiidae		
Calanidae		
Calocalanus pavo		
Candaciidae		
Centropagidae		
Eucalanidae		
Euchaetidae		
Heterorhabdidae		
Metridinidae		
Pontellidae		
Pontellina plumata		
Monstrilloida		
Temoridae		
Oithonidae		
Harpacticoida		
Corycaeidae		
Oncaeidae		
Sapphirinidae		
Copilia		
Lubbockia		

crustacea

grazers

copepoda

omnivorous

Siphonostomatoida		
badfocus < Copepoda		
damaged < Copepoda		
multiple < Copepoda		
Crustacea	crustacea	predators
Eumalacostraca		
Amphipoda		
Caprellidae		
Gammaridea		
protozoa		
Hyperidea		
Brachyura		
Phronimidae		
megalopa		
zoea < megalopa		
Euphausiacea		
calyptopsis < Euphausiacea		
Isopoda		
Laomediidae		
larvae < Porcellanidae		
phyllosoma		
nauplii < Crustacea	crustacea	grazers
metanauplii < Crustacea		
Ostracoda		
larvae < Squillidae		
Cyanobacteria < Bacteria	cyanobacteria	autotroph
Echinodermata	other	grazers
echinopluteus		
pluteus < echinoidea		
ophiuroida		
ophiopluteus		
pluteus<ophiuroida		
Harosa	rhizaria	mixotroph
Acantharia		
Collodaria		
Globorotalidae		

Orbunila		
Foraminifera		
Spumellaria		
Pyrocystaceae	dinoflagellata	mixotroph
multiple < Pyrocystaceae		
Insecta	other	predators
Halobates		
Mollusca	mollusca	grazers
Bivalva		
Gymnosomata		
Cavolinia inflexa		
Diacria		
Atlanta		
Cavoliniidae		
Cephalopoda		
Creseidae		
Creseis acicula		
Creseis virgula		
Firola		
Limacinidae		
part < Mollusca		
veliger		
Doliolida	tunicata	predators
Salpida		
juvenil < Salpida		
nucleus < Salpida		
egg < other	other	_
egg sac < egg		
gelatinous	other	predators
nudibranchia	other	_
multiple < other	other	_
othertocheck	other unidentified	unidentified

darksphere		
othersphere		
t001	other unidentified	unidentified
t002		
t003		
t004		
part < Actinopterygii	non-living	-
scale < Actinopterygii		
trunk < Appendicularia		
head < Chaetognatha		
part < Annelida		
tail < Appendicularia		
tail < Chaetognatha		
part < Thaliacea		
part < Siphonophorae		
part < Copepoda		
part < Cnidaria		
part < Crustacea		
part < Ctenophora		
wing < Halobates		
empty < Ostracoda		
artefact		
badfocus < artefact		
bubble		
detritus		
borax		
dark < detritus		
fiber < detritus		

919

920 **Table A3. List of EcoTaxa taxonomic annotations and associated groups: plankton groups and trophic type for the**
921 **ZooScan HSN 330 microns dataset.**

922

Tara Pacific 2016 2018 Manta 300 plankton		
Taxonomic list	Plankton groups	Trophic type
Actinopterygii	other	predators
egg < Actinopterygii		
Annelida	other	omnivorous
larvae < Annelida		

Alciopidae		
Tomopteridae		
Spirorbis		
Terebellidae		
Fritillariidae	tunicata	grazers
Oikopleuridae		
Chaetognatha	chaetognatha	predators
Cnidaria		
polype < Anthozoa		
Hydrozoa		
larvae < Porpitidae		
Porpita porpita		
Velella		
polype < Leptothecata		
bract < Abylopsis tetragona		
eudoxie < Abylopsis tetragona		
gonophore < Abylopsis tetragona		
nectophore < Abylopsis tetragona		
bract < Bassia bassensis		
gonophore < Bassia bassensis		
nectophore < Bassia bassensis		
bract < Diphyidae		
Chelophyes		
eudoxie < Diphyidae		
eudoxie < Eudoxoides spiralis		
gonophore < Eudoxoides spiralis		
nectophore < Eudoxoides spiralis		
gonophore < Diphyidae		
nectophore < Diphyidae		
nectophore < Hippopodiidae		
Physalia		
nectophore < Physonectae		
Aglaura		
Rhopalonema velatum		
ephyra		
Ctenophora	other	predators

cirrus	crustacea	grazers
cypris		
nauplii < Cirripedia		
Evadne		
larvae < Crustacea		
metanauplii < Crustacea		
Eumalacostraca	crustacea	predators
Amphipoda		
Gammaridea		
Hyperiidea		
Oxycephalidae		
Phronima		
protozoa < Penaeidae		
protozoa < Sergestidae		
zoa < Galatheidae		
larvae < Porcellanidae		
Brachyura		
megalopa		
zoa < Brachyura		
like < Laomedidae		
calyptopsis		
protozoa < Mysida		
Crustacea	crustacea	predators
nauplii < Crustacea		
metanauplii < Crustacea		
Ostracoda		
larvae < Squillidae		grazers
Copepoda	copepoda	omnivorous
Calanoida		
Acartiidae		
Haloptilus		
Calanidae		
Candaciidae		
Centropagidae		
Eucalanidae		
Euchaetidae		
Metridinidae		
Calocalanus pavo		

Pontellidae		
Pontellina plumata		
Temoridae		
Oithonidae		
Harpacticoida		
Miraciidae		
Corycaeidae		
Lubbockia		
Oncaeidae		
Sapphirinidae		
Copilia		
badfocus < Copepoda		
multiple < Copepoda		
damaged < Copepoda		
Insecta	other	predators
Gerridae		
Bryozoa	other	grazers
cyphonaute		
Branchiostoma lanceolatum	other	grazers
Doliolida		
Pyrosomatida		
Salpida	tunicata	omnivorous
chain < Salpida		
juvenile < Salpida		
Mollusca		
Bivalvia		
Cephalopoda		
Atlanta		
Firola		
Gymnosomata	mollusca	grazers
Cavoliniidae		
Diacavolinia		
Diacria trispinosa		
Creseidae		
Creseis acicula		
Creseis virgula		

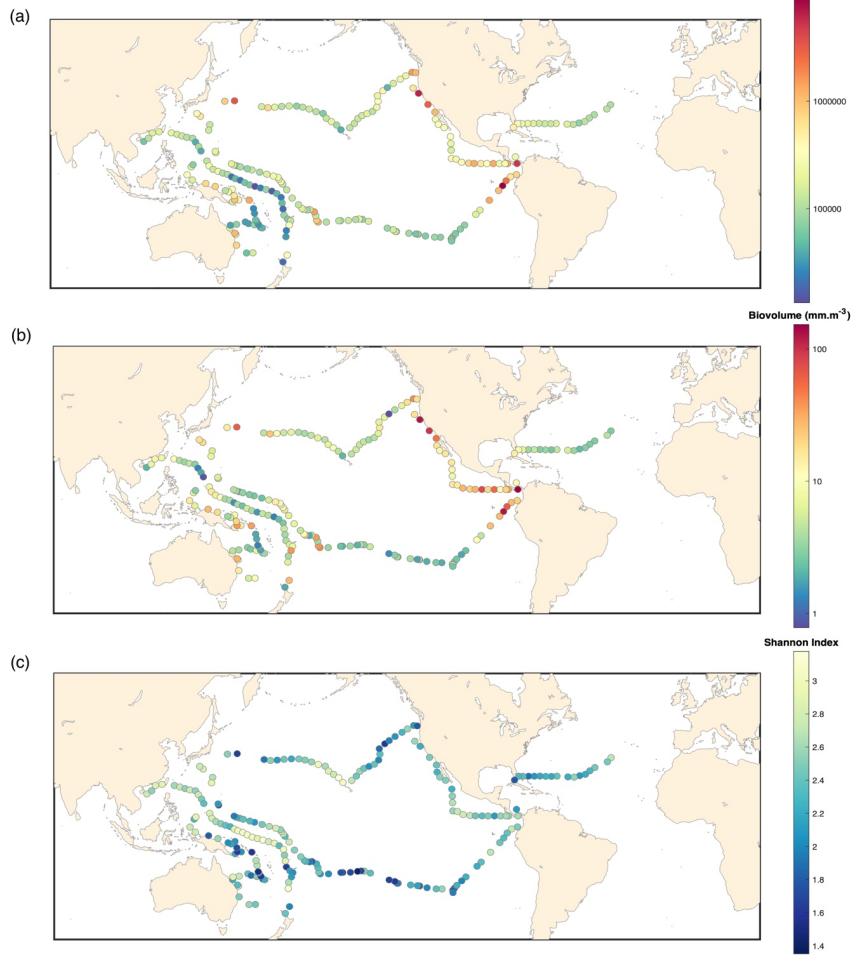
Limacinidae		
Nudibranchia		
egg < Mollusca	other	–
pluteus < Echinoidea	other	omnivorous
pluteus < Ophiuroidea		
Harosa	other	mixotroph
Neoceratium	dinoflagellata	
Pyrocystaceae		
Foraminifera	rhizaria	
Orbulina		
Spumellaria		
Diatoma	diatoms	phototroph
egg < other	other	–
living < other	other	–
multiple < other	other	–
othertocheck	other unidentified	unidentified
seaweed	other	phototroph
t002	other unidentified	unidentified
t003		
t004		
t005		
t007		
t008		
t010		
t012		
t013		
t014		
t015		
t016		
t017		
plastic<fiber	plastics	–
plastic<filament		

plastic<film		
plastic<fragment		
plastic<multiple		
plastic<other		
plastic<pellet		
plastic<polystyrene		
part<Copepoda	non-living	-
part<other		
scale<Actinopterygii		
part<Annelida		
tail<Appendicularia		
trunk<Appendicularia		
head<Chaetognatha		
tail<Chaetognatha		
part<Siphonophorae		
part<Cnidaria		
part<Ctenophora		
part<Crustacea		
wing<Insecta		
part<Thaliacea		
nucleus<Salpida		
part<Mollusca		
detritus		
artefact		
badfocus<artefact		
bubble		
dark<detritus		
fiber<detritus		

923

924 Table A4. List of EcoTaxa taxonomic annotations and associated groups: plankton groups and trophic type for the
925 ZooScan Manta 333 microns dataset.

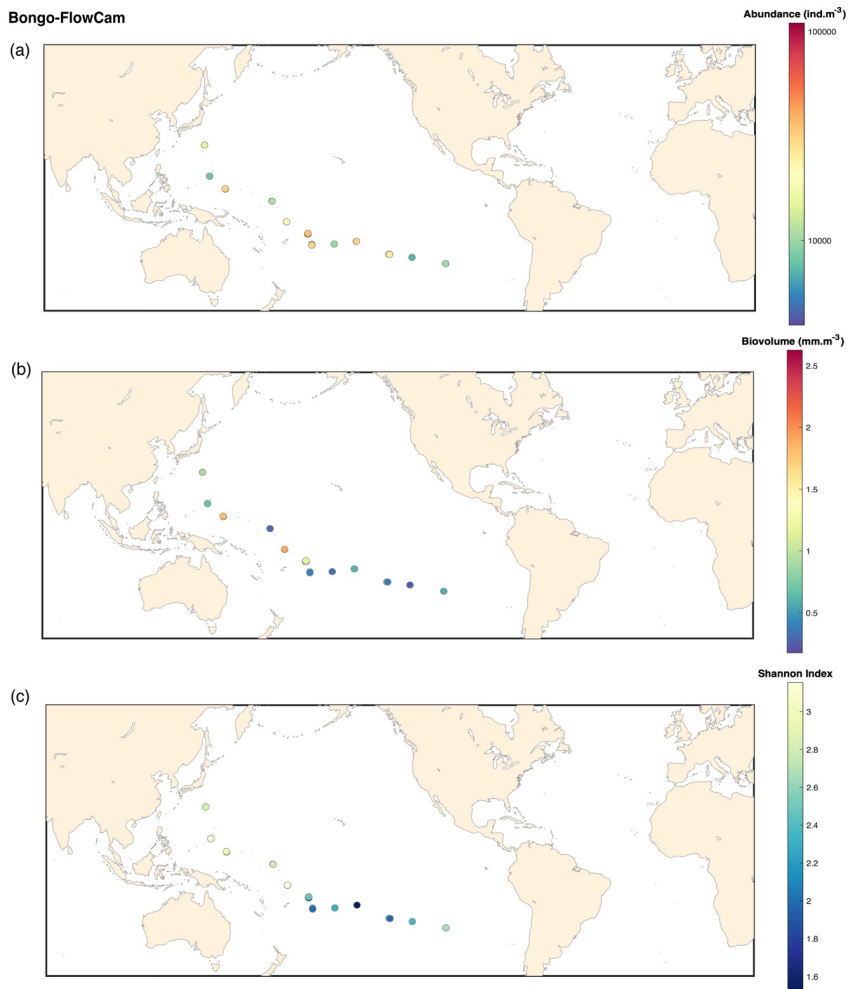
DN-FlowCam



926 Figure B1. FlowCam DN 20 microns: (a) Map of plankton abundance (ind.m⁻³). (b) Map of plankton biovolume (mm.m⁻³). (c) Map of Shannon diversity Index.
927
928

929

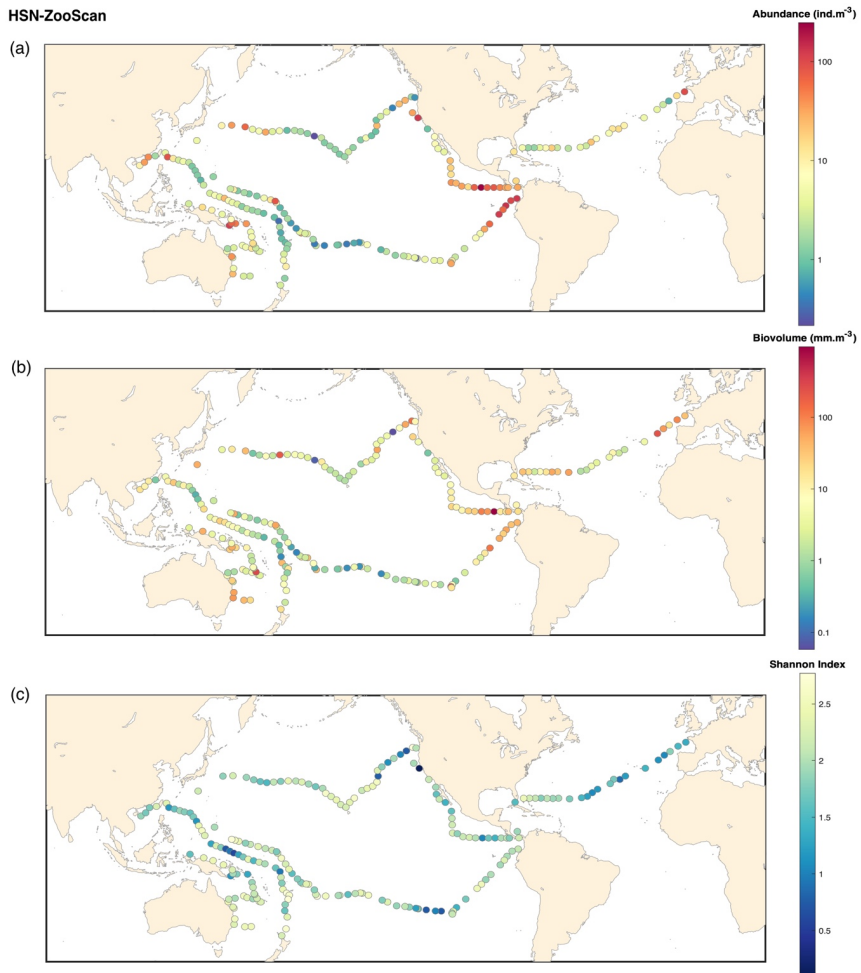
Bongo-FlowCam



930

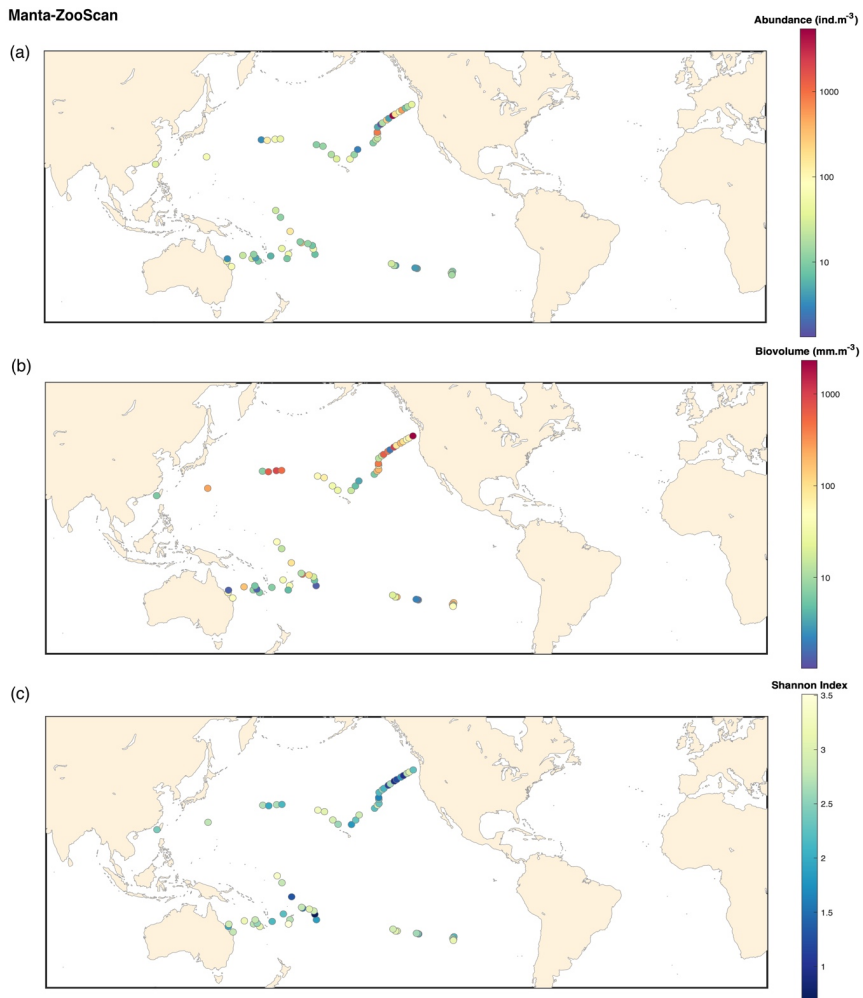
931 Figure B2. FlowCam Bongo 20 microns: (a) Map of plankton abundance (ind.m⁻³). (b) Map of plankton biovolume
932 (mm.m⁻³). (c) Map of Shannon diversity Index.

HSN-ZooScan

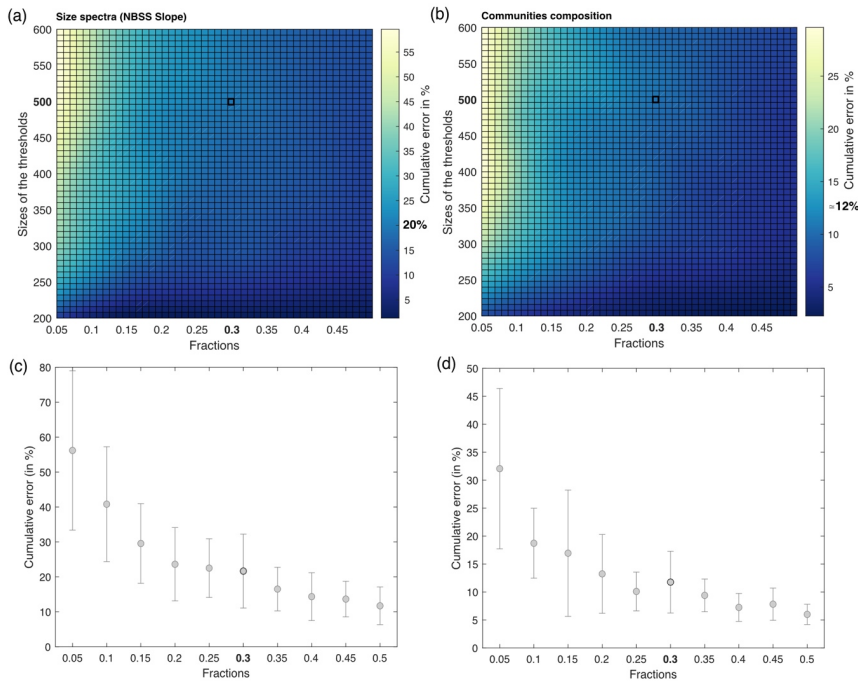


933 Figure B3. ZooScan HSN 330 microns: (a) Map of plankton abundance (ind.m⁻³). (b) Map of plankton biovolume
934 (mm.m⁻³). (c) Map of Shannon diversity Index.
935
936

Manta-ZooScan



937
938 Figure B4. ZooScan Manta 333 microns: (a) Map of plankton abundance (ind.m⁻³). (b) Map of plankton biovolume
939 (mm.m⁻³). (c) Map of Shannon diversity Index.



940

941 **Figure 4. (a) and (b) Estimated cumulative error associated with partial validation of particles below a size cut-off**
 942 **threshold ranging from 200 to 600 pixels and validated fractions ranging from 5% to 50%. Errors are computed as the**
 943 **percentage Root Mean Squared Error (RMSE) between fully validated samples and partially validated samples in**
 944 **three different metrics for cumulative error in respectively, NBSS slope and communities composition (relative**
 945 **abundance). RMSE values represent the outcomes of simulations, each conducted three times for the four samples,**
 946 **with random sampling. (c) and (d) Cumulative error according to the Fractions chosen in respectively, NBSS slope and**
 947 **communities composition. The threshold is fixed at 500 pixels.**

948 **Team list**

949 Tara Pacific Consortium Coordinators:

950
 951 Sylvain Agostini⁵, Denis Allemand⁶, Bernard Banaigs⁷, Emilie Boissin⁷, Emmanuel Boss³, Chris Bowler⁸,
 952 Colombar De Vargas⁹, Eric Douville¹⁰, Michel Flores¹¹, Didier Forcioli¹², Paola Furla¹², Pierre Galand¹³, Eric
 953 Gilson¹⁴, Stéphane Pesant¹⁵, Serge Planes¹⁶, Stéphanie Reynaud¹⁷, Matthew B. Sullivan¹⁸, Shinichi Sunagawa¹⁹,
 954 Olivier Thomas²⁰, Romain Troublé²¹, Rebecca Vega Thruher²², Christian R. Voolstra²³, Patrick Wincker²⁴, Didier
 955 Zoccola⁶

956 ⁵Shimoda Marine Research Center, University of Tsukuba, 5-10-1, Shimoda, Shizuoka, Japan

957 ⁶Centre Scientifique de Monaco, 8 Quai Antoine 1er, MC-98000, Principality of Monaco

958 ⁷PSL Research University: EPHE-UPVD-CNRS, USR 3278 CRIOBE, Université de Perpignan, France

959 ⁸Institut de Biologie de l'Ecole Normale Supérieure (IBENS), Ecole normale supérieure, CNRS, INSERM,
 960 Université PSL, 75005 Paris, France

961 ⁹Sorbonne Université, CNRS, Station Biologique de Roscoff, AD2M, UMR 7144, ECOMAP 29680 Roscoff,
 962 France

963 ¹⁰Laboratoire des Sciences du Climat et de l'Environnement, LSCE/IPSL, CEA-CNRS-UVSQ, Université Paris-
 964 Saclay, F-91191 Gif-sur-Yvette, France

965 ¹¹Weizmann Institute of Science, Department of Earth and Planetary Sciences, 76100 Rehovot, Israel

966 ¹²Université Côte d'Azur, CNRS, INSERM, IRCAN, Medical School, Nice, France and Department of Medical
967 Genetics, CHU of Nice, France
968 ¹³Sorbonne Université, CNRS, Laboratoire d'Ecogéochimie des Environnements Benthiques (LECOB),
969 Observatoire Océanologique de Banyuls, 66650 Banyuls sur mer, France
970 ¹⁴Université Côte d'Azur, CNRS, Inserm, IRCAN, France
971 ¹⁵European Molecular Biology Laboratory, European Bioinformatics Institute, Wellcome Genome Campus,
972 Hinxton, Cambridge CB10 1SD, UK
973 ¹⁶PSL Research University: EPHE-UPVD-CNRS, USR 3278 CRIOBE, Laboratoire d'Excellence CORAIL,
974 Université de Perpignan, 52 Avenue Paul Alduy, 66860 Perpignan Cedex, France
975 ¹⁷Centre Scientifique de Monaco, 8 Quai Antoine Ier, MC-98000, Principality of Monaco
976 ¹⁸The Ohio State University, Departments of Microbiology and Civil, Environmental and Geodetic Engineering,
977 Columbus, Ohio, 43210 USA
978 ¹⁹Department of Biology, Institute of Microbiology and Swiss Institute of Bioinformatics, Vladimir-Prelog-Weg
979 4, ETH Zürich, CH-8093 Zürich, Switzerland
980 ²⁰Marine Biodiscovery Laboratory, School of Chemistry and Ryan Institute, National University of Ireland,
981 Galway, Ireland
982 ²¹Fondation Tara Océan, Base Tara, 8 rue de Prague, 75 012 Paris, France
983 ²²Oregon State University, Department of Microbiology, 220 Nash Hall, 97331 Corvallis OR USA
984 ²³Department of Biology, University of Konstanz, 78457 Konstanz, Germany
985 ²⁴Génomique Métabolique, Genoscope, Institut François Jacob, CEA, CNRS, Univ Evry, Université Paris-Saclay,
986 91057 Evry, France

987 **Author contribution**

988 Conceptualization and methodology: Tara Pacific Consortium; GB, GG, SA, DA, BB, EB, EB, CB, CDV, ED,
989 MF, DF, PF, PG, EG, SP, SR, MBS, SS, OT, RT, RVT, CRV, PW, DZ, FL. Samples collection: GB, MLP, AE,
990 GG. Samples analysis (on lab) and investigation: ZM, NK, LJ, OB, LC, JM, AE. Data analysis, curation and
991 validation: ZM, NK, GB, LJ, MLP, MP, AE, LKB, FL. Supervision: GG, MLP, LKB, FL. Funding acquisition,
992 project administration and resources: FL, GG, MLP, LKB, GB, SA, DA, BB, EB, EB, CB, CDV, ED, MF, DF,
993 PF, PG, EG, SP, SR, MBS, SS, OT, RT, RVT, CRV, PW, DZ. Software: MP, ZM, GB, FL. Visualization and
994 Writing – original draft preparation: ZM, GB, GG, FL, MP. All authors have read and reviewed the manuscript.

995 **Competing interest**

996 The authors declare that they have no conflict of interest.

997 **Acknowledgment**

998
999 Special thanks to the Tara Ocean Foundation, the R/V Tara crew and the Tara Pacific Expedition Participants
1000 (<https://doi.org/10.5281/zenodo.3777760>). We are keen to thank the commitment of the following institutions for
1001 their financial and scientific support that made this unique Tara Pacific Expedition possible: CNRS, PSL, CSM,
1002 EPHE, Genoscope, CEA, Inserm, Université Côte d'Azur, ANR, agnès b., UNESCO-IOC, the Veolia Foundation,
1003 the Prince Albert II de Monaco Foundation, Région Bretagne, Billerudkorsnas, AmerisourceBergen Company,
1004 Lorient Agglomération, Oceans by Disney, L'Oréal, Biotherm, France Collectivités, Fonds Français pour
1005 l'Environnement Mondial (FFEM), Etienne Bourgeois, and the Tara Ocean Foundation teams. Tara Pacific would
1006 not exist without the continuous support of the participating institutes. The authors also particularly thank Serge
1007 Planes, Denis Allemand, and the Tara Pacific consortium. We thank the EMBRC collection CCPv for sample
1008 storage. This work was supported by EMBRC-France, whose French state funds are managed by the ANR within
1009 the Investments of the Future program under reference ANR-10-INBS-02. Support was also provided by the US
1010 National Science Foundation (NSF Biological Oceanography program (grant #2025402 to LKB) and the NASA
1011 Ocean Biology and Biogeochemistry program (grants #80NSSC20K1641). FL was also funded by the Institut
1012 Universitaire de France and co-funding by the European Union BIOcean5D GA#101059915 and the European

1013 Union's Horizon 2020 research and innovation programme "Atlantic Ecosystems Assessment, Forecasting and
1014 Sustainability" (AtlantECO) Grant ID: 862923. FL, OB, ZM are also funded by the ANR grant SmartBiodiv (grant
1015 ANR-21-AAFI-0002). This is publication number XX of the Tara Pacific Consortium. The authors particularly
1016 thank the Villefranche-sur-Mer Quantitative Imaging Platform (PIQv). Views and opinions expressed are however
1017 those of the author(s) only and do not necessarily reflect those of the European Union. Neither the European Union
1018 nor the granting authority can be held responsible for them.

1019 References

- 1020 Anraku, M. Some experiments on the variability of horizontal plankton hauls and on the horizontal distribution
1021 of plankton in limited area. *Bull. Fac. Fisheries, Hokkaido Univ.*, 7: 1-16, 1956.
- 1022 Barrows, A. P. W., Cathey, S. E., and Petersen, C. W.: Marine environment microfiber contamination: Global
1023 patterns and the diversity of microparticle origins, *Environmental Pollution*, 237, 275–284,
1024 <https://doi.org/10.1016/j.envpol.2018.02.062>, 2018.
- 1025 [Balachandran, T and Peter, K J. The role of plankton research in fisheries development, CMFRI Bulletin : National
1026 Symposium on Research and Development in Marine Fisheries Sessions I & II 1987, pp. 163-173, 1987.](#)
- 1027 Barnes, H. and Marshall, S. M., On the variability of replicate plankton samples and some applications of
1028 "contagious" series to statistical distributions of catches over restricted periods, *J. mar. biol. Ass. U.K.*, 1951.
- 1029 Bax, N. J., Miloslavich, P., Muller-Karger, F. E., Allain, V., Appeltans, W., Batten, S. D., Benedetti-Cecchi, L.,
1030 Buttigieg, P. L., Chiba, S., Costa, D. P., Duffy, J. E., Dunn, D. C., Johnson, C. R., Kudela, R. M., Obura, D.,
1031 Rebelo, L.-M., Shin, Y.-J., Simmons, S. E., and Tyack, P. L.: A Response to Scientific and Societal Needs for
1032 Marine Biological Observations, *Front. Mar. Sci.*, 6, 395, <https://doi.org/10.3389/fmars.2019.00395>, 2019.
- 1033 Beaugrand, G.: Monitoring pelagic ecosystems using plankton indicators, *ICES Journal of Marine Science*, 62,
1034 333–338, <https://doi.org/10.1016/j.icesjms.2005.01.002>, 2005.
- 1035 Belsler, C., Poulain, J., Labadie, K., Gavory, F., Alberti, A., Guy, J., Carradec, Q., Cruaud, C., Da Silva, C.,
1036 Engelen, S., Mielle, P., Perdereau, A., Samson, G., Gas, S., Genoscope Technical Team, Batisse, J., Beluche, O.,
1037 Bertrand, L., Bohers, C., Bordelais, I., Brun, E., Dubois, M., Dumont, C., Zineb, E. H., Estrada, B., Etedgui, E.,
1038 Fernandez, P., Garidi, S., Guérin, T., Gorrichon, K., Hamon, C., Kientzel, L., Lebled, S., Legrain, C., Lenoble,
1039 P., Lepretre, M., Louesse, C., Magdelenat, G., Mahieu, E., Martins, N., Milani, C., Orvain, C., Oztas, S., Payen,
1040 E., Petit, E., Rio, G., Robert, D., Ronsin, M., Vacherie, B., Voolstra, C. R., Galand, P. E., Flores, J. M., Hume, B.,
1041 C. C., Perna, G., Ziegler, M., Ruscheweyh, H.-J., Boissin, E., Romac, S., Bourdin, G., Iwankow, G., Moulin, C.,
1042 Paz García, D. A., Agostini, S., Banaigs, B., Boss, E., Bowler, C., De Vargas, C., Douville, E., Forcioli, D., Furla,
1043 P., Gilson, E., Lombard, F., Pesant, S., Reynaud, S., Sunagawa, S., Thomas, O. P., Troublé, R., Thurber, R. V.,
1044 Zoccola, D., Scarpelli, C., Jacoby, E. K., Oliveira, P. H., Aury, J.-M., Allemand, D., Planes, S., and Wincker, P.:
1045 Integrative omics framework for characterization of coral reef ecosystems from the Tara Pacific expedition, *Sci
1046 Data*, 10, 326, <https://doi.org/10.1038/s41597-023-02204-0>, 2023.
- 1047 Bopp, L., Resplandy, L., Orr, J. C., Doney, S. C., Dunne, J. P., Gehlen, M., Halloran, P., Heinze, C., Ilyina, T.,
1048 Séférian, R., Tjiputra, J., and Vichi, M.: Multiple stressors of ocean ecosystems in the 21st century: projections
1049 with CMIP5 models, *Biogeosciences*, 10, 6225–6245, <https://doi.org/10.5194/bg-10-6225-2013>, 2013.
- 1050 Borkman, D. G. and Smayda, T. J.: Gulf Stream position and winter NAO as drivers of long-term variations in
1051 the bloom phenology of the diatom *Skeletonema costatum* "species-complex" in Narragansett Bay, RI, USA,
1052 *Journal of Plankton Research*, 31, 1407–1425, <https://doi.org/10.1093/plankt/fbp072>, 2009.
- 1053 Bourdin, G., Karp-Boss, L., Lombard, F., Gorsky, G., and Boss, E.: Dynamic island mass effect from space. Part
1054 I: detecting the extent, <https://doi.org/10.5194/egusphere-2024-2670>, 15 October 2024.
- 1055 Bourdin, Lombard, Boss, Douville, Flores, Cassar, Cohen, Dimier, Fin, Gorsky, John, Kelly, Koren, Lin, Marie,
1056 Metz, Pujo-Pay, Ras, Reverdin, Vardi, Conan, Ghiglione, Moulin, Boissin, Iwankow, Poulain, Romac, Agostini,
1057 Banaigs, Bowler, De Vargas, Forcioli, Furla, Galand, P. E., Gilson, E., Pesant, S., Reynaud, S., Sullivan, M. B.,
1058 Sunagawa, S., Thomas, O., Troublé, R., Vega Thurber, R., Voolstra, C. R., Wincker, P., Zoccola, D., Allemand,
1059 D., and Planes, S.: Environmental context observed during the Tara Pacific Expedition 2016-2018, simplified
1060 version at site level (1), <https://doi.org/10.5281/ZENODO.6474974>, 2022.

a supprimé :

1062 Chavez, F. P., Messié, M., and Pennington, J. T.: Marine Primary Production in Relation to Climate Variability
1063 and Change, *Annu. Rev. Mar. Sci.*, 3, 227–260, <https://doi.org/10.1146/annurev.marine.010908.163917>, 2011.

1064 Checkley, D. M. and Barth, J. A.: Patterns and processes in the California Current System, *Progress in*
1065 *Oceanography*, 83, 49–64, <https://doi.org/10.1016/j.pocean.2009.07.028>, 2009.

1066 Cook, K. B.: Comparison of the epipelagic zooplankton samples from a U-Tow and the traditional WP2 net,
1067 *Journal of Plankton Research*, 23, 953–962, <https://doi.org/10.1093/plankt/23.9.953>, 2001.

1068 Copepod data base: <https://www.st.nmfs.noaa.gov/copepod/>, last access: 12 November 2024.

1069 De Vargas, C., Le Bescot, N., Pollina, T., Henry, N., Romac, S., Colin, S., Haëntjens, N., Carmichael, M., Berger,
1070 C., Le Guen, D., Decelle, J., Mahé, F., Poulain, J., Malpot, E., Beaumont, C., Hardy, M., Guiffant, D., Probert, I.,
1071 Gruber, D. F., Allen, A. E., Gorsky, G., Follows, M. J., Pochon, X., Troublé, R., Cael, B. B., Lombard, F., Boss,
1072 E., Prakash, M., and the Plankton Planet core team: Plankton Planet: A frugal, cooperative measure of aquatic life
1073 at the planetary scale, *Front. Mar. Sci.*, 9, 936972, <https://doi.org/10.3389/fmars.2022.936972>, 2022.

1074 Drago, L., Panaïotis, T., Irissou, J.-O., Babin, M., Biard, T., Carlotti, F., Coppola, L., Guidi, L., Hauss, H., Karp-
1075 Boss, L., Lombard, F., McDonnell, A. M. P., Picheral, M., Rogge, A., Waite, A. M., Stemmann, L., and Kiko, R.:
1076 Global Distribution of Zooplankton Biomass Estimated by In Situ Imaging and Machine Learning, *Front. Mar.*
1077 *Sci.*, 9, 894372, <https://doi.org/10.3389/fmars.2022.894372>, 2022.

1078 [Elton, C.: *Animal ecology*, 207 pp. Sidgwick Jackson LTD Lond., 1927.](https://doi.org/10.1016/j.joule.2019.07.001)

1079 Eriksen, M. B. and Frandsen, T. F.: The impact of patient, intervention, comparison, outcome (PICO) as a search
1080 strategy tool on literature search quality: a systematic review, *jmla*, 106, <https://doi.org/10.5195/jmla.2018.345>,
1081 2018.

1082 Falkowski, P. G., Fenchel, T., and Delong, E. F.: The Microbial Engines That Drive Earth's Biogeochemical
1083 Cycles, *Science*, 320, 1034–1039, <https://doi.org/10.1126/science.1153213>, 2008.

1084 Gorsky, G., Ohman, M. D., Picheral, M., Gasparini, S., Stemmann, L., Romagnan, J.-B., Cawood, A., Pesant, S.,
1085 Garcia-Comas, C., and Prejger, F.: Digital zooplankton image analysis using the ZooScan integrated system,
1086 *Journal of Plankton Research*, 32, 285–303, <https://doi.org/10.1093/plankt/fbp124>, 2010.

1087 Gorsky, G., Bourdin, G., Lombard, F., Pedrotti, M. L., Audrain, S., Bin, N., Boss, E., Bowler, C., Cassar, N.,
1088 Caudan, L., Chabot, G., Cohen, N. R., Cron, D., De Vargas, C., Dolan, J. R., Douville, E., Elineau, A., Flores, J.
1089 M., Ghiglione, J. F., Haëntjens, N., Hertau, M., John, S. G., Kelly, R. L., Koren, I., Lin, Y., Marie, D., Moulin,
1090 C., Moucherie, Y., Pesant, S., Picheral, M., Poulain, J., Pujo-Pay, M., Reverdin, G., Romac, S., Sullivan, M. B.,
1091 Trainic, M., Tressol, M., Troublé, R., Vardi, A., Voolstra, C. R., Wincker, P., Agostini, S., Banaigs, B., Boissin,
1092 E., Forcioli, D., Furla, P., Galand, P. E., Gilson, E., Reynaud, S., Sunagawa, S., Thomas, O. P., Thurber, R. L. V.,
1093 Zoccola, D., Planes, S., Allemand, D., and Karsenti, E.: Expanding Tara Oceans Protocols for Underway,
1094 Ecosystemic Sampling of the Ocean-Atmosphere Interface During Tara Pacific Expedition (2016–2018), *Front.*
1095 *Mar. Sci.*, 6, 750, <https://doi.org/10.3389/fmars.2019.00750>, 2019.

1096 Gove, J. M., McManus, M. A., Neuheimer, A. B., Polovina, J. J., Drazen, J. C., Smith, C. R., Merrifield, M. A.,
1097 Friedlander, A. M., Ehses, J. S., Young, C. W., Dillon, A. K., and Williams, G. J.: Near-island biological hotspots
1098 in barren ocean basins, *Nat Commun*, 7, 10581, <https://doi.org/10.1038/ncomms10581>, 2016.

1099 [Guo, C., Fu, C., Forrest, R. E., Olsen, N., Liu, H., Verley, P., and Shin, Y.-J.: Ecosystem-based reference points
1100 under varying plankton productivity states and fisheries management strategies, *ICES Journal of Marine Science*,
1101 *76*, 2045–2059, <https://doi.org/10.1093/icesjms/fsz120>, 2019.](https://doi.org/10.1016/j.joule.2019.07.001)

1102 Harris, R., Wiebe, P., Lenz, S., Skjoldal, H. R., Huntley, M.: *ICES Zooplankton Methodology Manual*, Elsevier,
1103 <https://doi.org/10.1016/B978-0-12-327645-2.X5000-2>, 2000.

1104 [Hays, G., Richardson, A., and Robinson, C.: Climate change and marine plankton, *Trends in Ecology & Evolution*,
1105 *20*, 337–344, <https://doi.org/10.1016/j.tree.2005.03.004>, 2005.](https://doi.org/10.1016/j.tree.2005.03.004)

1106 [Helm, R. R.: The mysterious ecosystem at the ocean's surface, *PLoS Biol.*, *19*, e3001046,
1107 <https://doi.org/10.1371/journal.pbio.3001046>, 2021.](https://doi.org/10.1371/journal.pbio.3001046)

1108 Herdman, W.A., Variations in successive vertical plankton hauls at Port Erin. *Proc. And Trans. L'pool biol. Soc.*,
1109 Vol. 35, pp, 161-74, 1921.

1110 Hidalgo-Ruz, V., Gutow, L., Thompson, R. C., and Thiel, M.: Microplastics in the Marine Environment: A
1111 Review of the Methods Used for Identification and Quantification, *Environ. Sci. Technol.*, 46, 3060–3075,
1112 <https://doi.org/10.1021/es2031505>, 2012.

1113 [Ibarbalz, F. M., Henry, N., Brandão, M. C., Martini, S., Busseni, G., Byrne, H., Coelho, L. P., Endo, H., Gasol, J.](#)
1114 [M., Gregory, A. C., Mahé, F., Rigonato, J., Royo-Llonch, M., Salazar, G., Sanz-Sáez, I., Scalco, E., Soviadan, D.,](#)
1115 [Zayed, A. A., Zingone, A., Labadie, K., Ferland, J., Marec, C., Kandels, S., Picheral, M., Dimier, C., Poulain, J.,](#)
1116 [Pisarev, S., Carmichael, M., Pesant, S., Babin, M., Boss, E., Iudicone, D., Jaillon, O., Acinas, S. G., Ogata, H.,](#)
1117 [Pelletier, E., Stemmann, L., Sullivan, M. B., Sunagawa, S., Bopp, L., de Vargas, C., Karp-Boss, L., Wincker, P.,](#)
1118 [Lombard, F., Bowler, C., Zinger, L., Acinas, S. G., Babin, M., Bork, P., Boss, E., Bowler, C., Cochrane, G., de](#)
1119 [Vargas, C., Follows, M., Gorsky, G., Grimsley, N., Guidi, L., Hingamp, P., Iudicone, D., Jaillon, O., Kandels, S.,](#)
1120 [Karp-Boss, L., Karsenti, E., Not, F., Ogata, H., Pesant, S., Poulton, N., Raes, J., Sardet, C., Speich, S., Stemmann,](#)
1121 [L., Sullivan, M. B., Sunagawa, S., and Wincker, P.: Global Trends in Marine Plankton Diversity across Kingdoms](#)
1122 [of Life, Cell, 179, 1084-1097.e21, <https://doi.org/10.1016/j.cell.2019.10.008>, 2019.](#)
1123 [Intergovernmental Panel On Climate Change \(Ipc\): Climate Change 2022 – Impacts, Adaptation and](#)
1124 [Vulnerability: Working Group II Contribution to the Sixth Assessment Report of the Intergovernmental Panel on](#)
1125 [Climate Change, 1st ed., Cambridge University Press, <https://doi.org/10.1017/9781009325844>, 2023.](#)
1126 Ikeda, T.: Metabolic rates of epipelagic marine zooplankton as a function of body mass and temperature, *Mar.*
1127 *Biol.*, 85, 1–11, <https://doi.org/10.1007/BF00396409>, 1985.
1128 Imai, K. and Lehmann, H.: The oxygen affinity of haemoglobin Tak, a variant with an elongated beta chain,
1129 *Biochim Biophys Acta*, 412, 288–294, [https://doi.org/10.1016/0005-2795\(75\)90043-4](https://doi.org/10.1016/0005-2795(75)90043-4), 1975.
1130 Jalabert, L.: ZooScan Protocol v1, <https://doi.org/10.17504/protocols.io.yxmvmk8j9g3p/v1>, 27 October 2021.
1131 Jonas, T. D.: The volume of water filtered by a Continuous Plankton Recorder sample: the effect of ship speed,
1132 *Journal of Plankton Research*, 26, 1499–1506, <https://doi.org/10.1093/plankt/fbh137>, 2004.
1133 Karlsson, T. M., Kärrman, A., Rotander, A., and Hassellöv, M.: Comparison between manta trawl and in situ
1134 pump filtration methods, and guidance for visual identification of microplastics in surface waters, *Environ Sci*
1135 *Pollut Res*, 27, 5559–5571, <https://doi.org/10.1007/s11356-019-07274-5>, 2020.
1136 Keen, E.: A Practical Designer's Guide to Mesozooplankton Nets, Available:
1137 <http://acsweb.ucsd.edu/~ekeen/resources/Choosing-a-Net.pdf>, 2013, last access: 12 November 2024.
1138 [Lampert, W.: The Adaptive Significance of Diel Vertical Migration of Zooplankton, *Functional Ecology*, 3, 21,](#)
1139 <https://doi.org/10.2307/2389671>, 1989.
1140 Lombard, F., Boss, E., Waite, A. M., Vogt, M., Uitz, J., Stemmann, L., Sosik, H. M., Schulz, J., Romagnan, J.-
1141 B., Picheral, M., Pearlman, J., Ohman, M. D., Niehoff, B., Möller, K. O., Miloslavich, P., Lara-Lpez, A., Kudela,
1142 R., Lopes, R. M., Kiko, R., Karp-Boss, L., Jaffé, J. S., Iversen, M. H., Irisson, J.-O., Fennel, K., Hauss, H., Guidi,
1143 L., Gorsky, G., Giering, S. L. C., Gaube, P., Gallager, S., Dubelaar, G., Cowen, R. K., Carlotti, F., Briseño-Avena,
1144 C., Berline, L., Benoit-Bird, K., Bax, N., Batten, S., Ayata, S. D., Artigas, L. F., and Appeltans, W.: Globally
1145 Consistent Quantitative Observations of Planktonic Ecosystems, *Front. Mar. Sci.*, 6, 196,
1146 <https://doi.org/10.3389/fmars.2019.00196>, 2019.
1147 Gehring, J.W.: An all metal plankton sampler (model Gulf III), U.S. Fish and Wildl. Serv., spec. sci. Rep. Fish.,
1148 (88) 7-12, 1958.
1149 Lombard, F., Bourdin, G., Pesant, S., Agostini, S., Baudena, A., Boissin, E., Cassar, N., Clampitt, M., Conan, P.,
1150 Da Silva, O., Dimier, C., Douville, E., Elineau, A., Fin, J., Flores, J. M., Ghiglione, J.-F., Hume, B. C. C., Jalabert,
1151 L., John, S. G., Kelly, R. L., Koren, I., Lin, Y., Marie, D., McMinds, R., Mériguet, Z., Metzl, N., Paz-García, D.
1152 A., Pedrotti, M. L., Poulain, J., Pujó-Pay, M., Ras, J., Reverdin, G., Romac, S., Rouan, A., Röttinger, E., Vardi,
1153 A., Voolstra, C. R., Moulin, C., Iwankow, G., Banaigs, B., Bowler, C., De Vargas, C., Forcioli, D., Furla, P.,
1154 Galand, P. E., Gilson, E., Reynaud, S., Sunagawa, S., Sullivan, M. B., Thomas, O. P., Troublé, R., Thurber, R.
1155 V., Wincker, P., Zoccola, D., Allemand, D., Planes, S., Boss, E., and Gorsky, G.: Open science resources from
1156 the Tara Pacific expedition across coral reef and surface ocean ecosystems, *Sci Data*, 10, 324,
1157 <https://doi.org/10.1038/s41597-022-01757-w>, 2023.
1158 Longhurst, A. R.: TOWARD AN ECOLOGICAL GEOGRAPHY OF THE SEA, in: *Ecological Geography of the*
1159 *Sea*, Elsevier, 1–17, <https://doi.org/10.1016/B978-012455521-1/50002-4>, 2007.
1160 Longhurst, A. R., Reith, A. D., Bower, R. E., and Seibert, D. L. R.: A new system for the collection of multiple
1161 serial plankton samples, *Deep Sea Research and Oceanographic Abstracts*, 13, 213–222,
1162 [https://doi.org/10.1016/0011-7471\(66\)91101-6](https://doi.org/10.1016/0011-7471(66)91101-6), 1966.

1163 Picheral, M., Colin, S. and Irisson, J. O.: EcoTaxa, a tool for the taxonomic classification of images:
1164 <http://ecotaxa.obs-vlfr.fr>.

1165 Mériquet, Z., Bourdin, G., Jalabert, L., Caray--Counil, L., Maury, J., Elineau, A., Pedrotti, M.-L., Gorsky, G., and
1166 Lombard, F.: Global scale surface meso-plankton and microplastics dataset collected with Manta Net and imaged
1167 with ZooScan during the Tara Pacific Expedition, <https://doi.org/10.17882/102537>, 2024a.

1168 Mériquet, Z., Bourdin, G., Jalabert, L., Bun, O., Caray--Counil, L., Elineau, A., Gorsky, G., and Lombard, F.:
1169 Global scale surface meso-plankton dataset collected with High-Speed Net and imaged with ZooScan during the
1170 Tara Pacific Expedition, <https://doi.org/10.17882/102336>, 2024b.

1171 Mériquet, Z., Kristan, N., Bourdin, G., Gorsky, G., Karp-Boss, L., and Lombard, F.: Global scale surface micro-
1172 plankton dataset collected with Bongo nets and imaged with FlowCam during the Tara Pacific Expedition,
1173 <https://doi.org/10.17882/102694>, 2024c.

1174 Mériquet, Z., Bourdin, G., Jalabert, L., Bun, O., Caray--Counil, L., Elineau, A., Gorsky, G., and Lombard, F.:
1175 Global scale surface micro-plankton dataset collected with Deck Net and imaged with FlowCam during the Tara
1176 Pacific Expedition, <https://doi.org/10.17882/102697>, 2024d.

1177 Mériquet, Z., Oddone, A., Le Guen, D., Pollina, T., Bazile, R., Moulin, C., Troublé, R., Prakash, M., De Vargas,
1178 C., and Lombard, F.: Basin-Scale Underway Quantitative Survey of Surface Microplankton Using Affordable
1179 Collection and Imaging Tools Deployed From Tara, *Front. Mar. Sci.*, 9, 916025,
1180 <https://doi.org/10.3389/fmars.2022.916025>, 2022.

1181 Messié, M., Petrenko, A., Doglioli, A. M., Martinez, E., and Alvain, S.: Basin-scale biogeochemical and
1182 ecological impacts of islands in the tropical Pacific Ocean, *Nat. Geosci.*, 15, 469–474,
1183 <https://doi.org/10.1038/s41561-022-00957-8>, 2022.

1184 [Mignot, A., Claustre, H., Uitz, J., Poteau, A., D'Ortenzio, F., and Xing, X.: Understanding the seasonal dynamics
1185 of phytoplankton biomass and the deep chlorophyll maximum in oligotrophic environments: A Bio-Argo float
1186 investigation, *Global Biogeochemical Cycles*, 28, 856–876, <https://doi.org/10.1002/2013GB004781>, 2014.](https://doi.org/10.1002/2013GB004781)

1187 Motoda, S.: Devices of simple plankton apparatus, 1959.

1188 Pasquier, G., Doyen, P., Kazour, M., Dehaut, A., Diop, M., Duflos, G., and Amara, R.: Manta Net: The Golden
1189 Method for Sampling Surface Water Microplastics in Aquatic Environments, *Front. Environ. Sci.*, 10, 811112,
1190 <https://doi.org/10.3389/fenvs.2022.811112>, 2022.

1191 Pedrotti, M. L., Lombard, F., Baudena, A., Galgani, F., Elineau, A., Petit, S., Henry, M., Troublé, R., Reverdin,
1192 G., Ser-Giacomi, E., Kedzierski, M., Boss, E., and Gorsky, G.: An integrative assessment of the plastic debris
1193 load in the Mediterranean Sea, *Science of The Total Environment*, 838, 155958,
1194 <https://doi.org/10.1016/j.scitotenv.2022.155958>, 2022.

1195 Picheral, P., Colin, S. and Irisson, J. O.: EcoTaxa, a tool for the taxonomic classification of images:
1196 <http://ecotaxa.obs-vlfr.fr>, last access: 12 November 2024.

1197 Piqv site: <https://sites.google.com/view/piqv/piqvmanuals/instruments-manuals>, last access: 1 November 2024.

1198 Planes, S., Allemand, D., Agostini, S., Banaigs, B., Boissin, E., Boss, E., Bourdin, G., Bowler, C., Douville, E.,
1199 Flores, J. M., Forcioli, D., Furla, P., Galand, P. E., Ghiglione, J.-F., Gilson, E., Lombard, F., Moulin, C., Pesant,
1200 S., Poulain, J., Reynaud, S., Romac, S., Sullivan, M. B., Sunagawa, S., Thomas, O. P., Troublé, R., De Vargas,
1201 C., Vega Thurber, R., Woolstra, C. R., Wincker, P., Zoccola, D., and the Tara Pacific Consortium: The Tara Pacific
1202 expedition—A pan-ecosystemic approach of the “-omics” complexity of coral reef holobionts across the Pacific
1203 Ocean, *PLoS Biol*, 17, e3000483, <https://doi.org/10.1371/journal.pbio.3000483>, 2019.

1204 Platt, T., Denman, K.: The structure of pelagic ecosystems. *Rapp P-V Reun. Cons. Int. Explor Mer* 173:60-5,
1205 1978.

1206 [Robinson, K. L., Sponaugle, S., Luo, J. Y., Gleiber, M. R., and Cowen, R. K.: Big or small, patchy all: Resolution
1207 of marine plankton patch structure at micro- to submesoscales for 36 taxa, *Sci. Adv.*, 7, eabk2904,
1208 <https://doi.org/10.1126/sciadv.abk2904>, 2021.](https://doi.org/10.1126/sciadv.abk2904)

1209 Sameoto, D., Wiebe, P., Runge, J., Postel, L., Dunn, J., Miller, C., and Coombs, S.: Collecting zooplankton, in:
1210 *ICES Zooplankton Methodology Manual*, Elsevier, 55–81, <https://doi.org/10.1016/B978-012327645-2/50004-9>,
1211 2000.

1212 [Santiago, B. C. F., De Souza, I. D., Cavalcante, J. V. F., Morais, D. A. A., Da Silva, M. B., Pasquali, M. A. D. B.,
1213 and Dalmolin, R. J. S.: Metagenomic Analyses Reveal the Influence of Depth Layers on Marine Biodiversity on](https://doi.org/10.1016/j.cub.2021.08.001)

a mis en forme : Anglais (G.B.)

214 [Tropical and Subtropical Regions, *Microorganisms*, 11, 1668, <https://doi.org/10.3390/microorganisms11071668>,](https://doi.org/10.3390/microorganisms11071668)
215 [2023.](https://doi.org/10.3390/microorganisms11071668)

216 [Shannon, C. E., & Weaver, W. *The mathematical theory of communication*. University of Illinois Press, 1949.](#)

217 [Sheldon, R. W., Prakash, A., and Sutcliffe, W. H.: THE SIZE DISTRIBUTION OF PARTICLES IN THE](#)
218 [OCEAN1: PARTICLES IN THE OCEAN, *Limnol. Oceanogr.*, 17, 327–340,](#)
219 [https://doi.org/10.4319/lo.1972.17.3.0327, 1972.](https://doi.org/10.4319/lo.1972.17.3.0327)

220 [Sieracki, C., Sieracki, M., and Yentsch, C.: An imaging-in-flow system for automated analysis of marine](#)
221 [microplankton, *Mar. Ecol. Prog. Ser.*, 168, 285–296, <https://doi.org/10.3354/meps168285>, 1998.](#)

222 [Skjoldal, H. R., Prokopchuk, I., Bagoien, E., Dalpadado, P., Nesterova, V., Rønning, J., and Knutsen, T.:](#)
223 [Comparison of Juday and WP2 nets used in joint Norwegian–Russian monitoring of zooplankton in the Barents](#)
224 [Sea, *Journal of Plankton Research*, 41, 759–769, <https://doi.org/10.1093/plankt/fbz054>, 2019.](#)

225 [Skjoldal, H. R., Wiebe, P., Postel, L., Knutsen, T., Kaartvedt, S., and Sameoto, D.: Intercomparison of](#)
226 [zooplankton \(net\) sampling systems: Results from the ICES/GLOBEC sea-going workshop, *Progress in*](#)
227 [Oceanography, 108, 1–42, <https://doi.org/10.1016/j.pocean.2012.10.006>, 2013.](#)

228 [Smith, P.E., Counts, R.C., Cutter, R.I: Changes in filtering efficiency of plankton nets due to clogging under tow.,](#)
229 [1968a.](#)

230 [Smith, P. E., Tranter, D. J., Filtration performance D.J. Tranter \(Ed.\), *Monographs on oceanographic methodology*](#)
231 [2, Zooplankton sampling, UNESCO Press, Paris \(1968\), pp. 27-56, 1968b.](#)

232 [Steinberg, D. K. and Landry, M. R.: Zooplankton and the Ocean Carbon Cycle, *Annu. Rev. Mar. Sci.*, 9, 413–](#)
233 [444, <https://doi.org/10.1146/annurev-marine-010814-015924>, 2017.](#)

234 [Tranter, D.J., Heron, A.C.: Experiments on filtration in plankton nets *Australian Journal of Marine and Freshwater*](#)
235 [Research, 18, pp. 89-111, 1967.](#)

236 [Trebilco, R., Baum, J. K., Salomon, A. K., and Dulvy, N. K.: *Ecosystem ecology: size-based constraints on the*](#)
237 [pyramids of life, *Trends in Ecology & Evolution*, 28, 423–431, <https://doi.org/10.1016/j.tree.2013.03.008>, 2013.](#)

238 [Turner, J. T.: Zooplankton fecal pellets, marine snow, phytodetritus and the ocean’s biological pump, *Progress in*](#)
239 [Oceanography, 130, 205–248, <https://doi.org/10.1016/j.pocean.2014.08.005>, 2015a.](#)

240 [Vandromme, P., Stemmann, L., Garcia-Comas, C., Berline, L., Sun, X., and Gorsky, G.: Assessing biases in](#)
241 [computing size spectra of automatically classified zooplankton from imaging systems: A case study with the](#)
242 [ZooScan integrated system, *Methods in Oceanography*, 1–2, 3–21, <https://doi.org/10.1016/j.mio.2012.06.001>,](#)
243 [2012.](#)

244 [Von Ammon, U., Jeffs, A., Zaiko, A., Van Der Reis, A., Goodwin, D., Beckley, L. E., Malpot, E., and Pochon,](#)
245 [X.: A Portable Cruising Speed Net: Expanding Global Collection of Sea Surface Plankton Data, *Front. Mar. Sci.*,](#)
246 [7, 615458, <https://doi.org/10.3389/fmars.2020.615458>, 2020.](#)

247 [Wiebe, P. H., and Holland, W. R., PLANKTON PATCHINESS: EFFECTS ON REPEATED NET TOWS, 1968.](#)

248 [Wilkinson, M. D., Dumontier, M., Aalbersberg, Ij. J., Appleton, G., Axton, M., Baak, A., Blomberg, N., Boiten,](#)
249 [J.-W., Da Silva Santos, L. B., Bourne, P. E., Bouwman, J., Brookes, A. J., Clark, T., Crosas, M., Dillo, I., Dumon,](#)
250 [O., Edmunds, S., Evelo, C. T., Finkers, R., Gonzalez-Beltran, A., Gray, A. J. G., Groth, P., Goble, C., Grethe, J.](#)
251 [S., Heringa, J., 'T Hoen, P. A. C., Hooft, R., Kuhn, T., Kok, R., Kok, J., Lusher, S. J., Martone, M. E., Mons, A.,](#)
252 [Packer, A. L., Persson, B., Rocca-Serra, P., Roos, M., Van Schaik, R., Sansone, S.-A., Schultes, E., Sengstag, T.,](#)
253 [Slater, T., Strawn, G., Swertz, M. A., Thompson, M., Van Der Lei, J., Van Mulligen, E., Velterop, J.,](#)
254 [Waagmeester, A., Wittenburg, P., Wolstencroft, K., Zhao, J., and Mons, B.: The FAIR Guiding Principles for](#)
255 [scientific data management and stewardship, *Sci Data*, 3, 160018, <https://doi.org/10.1038/sdata.2016.18>, 2016.](#)
256

1257

a supprimer: ¶

Page 4 : [1] a supprimé Microsoft Office User 10/03/2025 11:33:00

Page 20 : [2] a supprimé Microsoft Office User 14/03/2025 08:26:00